Vertical profiles of O3 and NOx chemistry in the polluted nocturnal boundary layer in Phoenix, AZ: I. Field observations by long-path DOAS

S. Wang, R. Ackermann, J. Stutz

Atmos. Chem. Phys., 6, 2671–2693, 2006
www.atmos-chem-phys.net/6/2671/2006/

Atmospheric Chemistry and Physics

Vertical profiles of O_3 and NO_x chemistry in the polluted nocturnal boundary layer in Phoenix, AZ: I. Field observations by long-path DOAS

S. Wang, R. Ackermann, and J. Stutz

Department of Atmospheric and Oceanic Sciences, University of California, Los Angeles, CA, USA

Received: 18 October 2005 – Published in Atmos. Chem. Phys. Discuss.: 3 January 2006
Revised: 4 April 2006 – Accepted: 29 May 2006 – Published: 6 July 2006

Abstract. Nocturnal chemistry in the atmospheric boundary layer plays a key role in determining the initial chemical conditions for photochemistry during the following morning as well as influencing the budgets of O_3 and NO_2. Despite its importance, chemistry in the nocturnal boundary layer (NBL), especially in heavily polluted urban areas, has received little attention so far, which greatly limits the current understanding of the processes involved. In particular, the influence of vertical mixing on chemical processes gives rise to complex vertical profiles of various reactive trace gases and makes nocturnal chemistry altitude-dependent. The processing of pollutants is thus driven by a complicated, and not well quantified, interplay between chemistry and vertical mixing.

In order to gain a better understanding of the altitude-dependent nocturnal chemistry in the polluted urban environment, a field study was carried out in the downtown area of Phoenix, AZ, in summer 2001. Vertical profiles of reactive species, such as O_3, NO_2, and NO_3, were observed in the lowest 140 m of the troposphere throughout the night. The disappearance of these trace gas vertical gradients during the morning coincided with the morning transition from a stable NBL to a well-mixed convective layer. The vertical gradients of trace gas levels were found to be dependent on both surface NO_x emission strength and the vertical stability of the NBL. The vertical gradients of O_x, the sum of O_3 and NO_2, were found to be much smaller than those of O_3 and NO_2, revealing the dominant role of NO emissions followed by the O_3+NO reaction for the altitude-dependence of nocturnal chemistry in urban areas. Dry deposition, direct emissions, and other chemical production pathways of NO_2 also play a role for the O_x distribution. Strong positive vertical gradients of NO_3, that are predominantly determined by NO_3 loss near the ground, were observed. The vertical profiles of NO_3 and the calculated vertical profiles of its reservoir species (N_2O_5) confirm earlier model results suggesting complex vertical distributions of atmospheric denoxification processes during the night.

Correspondence to: J. Stutz
(jochen@atmos.ucla.edu)

1 Introduction

Nocturnal chemistry in the polluted urban boundary layer has received surprisingly little attention thus far, despite its significance in determining initial conditions for photochemistry during the following day. It is well known that daytime chemistry is driven by photolytic reactions involving nitrogen oxides (NO_x), hydrocarbons, and hydroxyl radicals (HO_x) that lead to the formation of O_3 and particles. In contrast, at night O_3 undergoes a net loss in the absence of sunlight through dry deposition, NO titration, and other chemical pathways. The difference in O_3 chemistry between day and night leads to a diurnal cycle of high daytime and low night-time O_3 levels in the boundary layer in both rural and urban areas (Aneja et al., 2000; Colbeck and Harrison, 1985; Van Dop et al., 1977). While OH chemistry becomes less important during night-time (Abram et al., 2000; Alicke et al., 2002; Smith et al., 2002), the nitrate radical (NO_3) as well as O_3 become the dominant oxidants determining the budget of NO_x and VOCs (Geyer, 2000; Jenkin and Clemitshaw, 2000; Sadanaga et al., 2003). In addition, nocturnal chemistry also influences the aerosol composition, for example, through the uptake of the NO_3 reservoir species, N_2O_5 (Dentener and Crutzen, 1993; Geyer, 2000).

The absence of solar radiation at night also leads to radiative cooling of the surface which inhibits turbulence and vertical mixing. As a result, a stable nocturnal boundary layer (NBL), which is capped by a relatively well-mixed residual layer (RL) with neutral stability, develops. Due to the weak vertical mixing, ground-level emissions in urban areas accumulate near the surface throughout the night (Doran et al., 2003; Garland and Branson, 1976; Pisano et al.,

Published by Copernicus GmbH on behalf of the European Geosciences Union.

1997). However, even in the stable NBL, trace gases are slowly transported vertically. During this slow transport, reactive compounds such as O_3 and NO undergo chemical transformations. Because the timescales of turbulent transport and chemical reactions are similar, nocturnal chemistry and vertical transport are closely linked, leading to complex vertical distributions of various trace gases and making nocturnal chemistry altitude dependent. The study of chemistry in the NBL, especially in polluted urban areas, is thus quite challenging (Geyer and Stutz, 2004a; Stutz et al., 2004b). The altitude dependence of both chemistry and vertical trace gas profiles vanish during the morning hours when surface heating leads to convection and accelerates vertical exchange (Doran et al., 2003; Garland and Branson, 1976; Pisano et al., 1997).

Few studies have thus far focused on the vertical variation of NBL chemistry. Night-time vertical distributions of O_3 have been measured in various rural and urban environments by tethered balloons, masts, and aircraft over a wide range of altitudes in the lower troposphere (Aneja et al., 2000; Chen et al., 2002; Colbeck and Harrison, 1985; Doran et al., 2003; Galbally, 1968; Glaser et al., 2003; Gusten et al., 1998; Harrison et al., 1978; Neu et al., 1994; Van Dop et al., 1977; Zhang and Rao, 1999). The results generally show positive vertical O_3 gradients, with higher O_3 concentrations at higher altitudes (Aneja et al., 2000; Galbally, 1968; Gusten et al., 1998; Van Dop et al., 1977; Zhang and Rao, 1999). Due to dry deposition (Colbeck and Harrison, 1985; Gusten et al., 1998; Harrison et al., 1978), reaction with surface emitted NO (Gusten et al., 1998), and inefficient vertical transport, O_3 is often depleted at the bottom of the NBL. O_3 above the nocturnal inversion is cut off from major sinks and is preserved at night. When the inversion begins to break up in the morning, rapid downward transport from the RL helps to restore the surface O_3 (Gusten et al., 1998; Kleinman et al., 1994; McKendry et al., 1997; Neu et al., 1994; Zhang and Rao, 1999). This has been confirmed by observations of a strong correlation between night-time O_3 in the RL and the maximum surface O_3 on the next day (Aneja et al., 2000; Zhang and Rao, 1999). Significant downward mixing of O_3 from the RL can contribute about half of the observed morning increase in surface O_3 concentrations in some cases (Kleinman et al., 1994; McKendry et al., 1997; Neu et al., 1994). In areas with good daytime ventilation to prohibit multi-day buildups of locally produced O_3, the impact of this downward mixing is significant even during the late day hours. The study of Fast et al. (2000) shows that the entrainment from the RL reservoir into the growing convective boundary layer could contribute 20 to 40% of the afternoon surface O_3 levels in Phoenix valley.

Recently, simultaneous measurements of multiple chemical species and meteorological parameters have been carried out to provide more information about the NBL. Vertical distribution measurements of O_3, NO_2, temperature and relative humidity in a suburban area show persistent vertical profiles for several hours after sunrise in some cases (Pisano et al., 1997). A similar trend has been found in the vertical profiles of O_3, NO_2, NO_x, selected VOCs and meteorological parameters after very stable nights at a rural site (Glaser et al., 2003). A field study near Houston, TX, revealed frequent negative NO_2 and positive O_3 vertical gradients when temperature inversions and calm wind conditions were encountered (Stutz et al., 2004b). In addition, NO_3 showed positive vertical gradients in the stable NBL (Stutz et al., 2004b), which agrees with earlier NO_3 measurements in the lower boundary layer (Aliwell and Jones, 1998; Friedeburg et al., 2002). Modeling studies attribute positive vertical gradients of both O_3 and NO_3 mainly to the reactions with surface-emitted NO and VOCs (Fish et al., 1999; Geyer and Stutz, 2004a; Stutz et al., 2004b). Vertical profiles of N_2O_5, which depend on temperature profiles as well as NO_2 and NO_3 distributions, also develop in the stable NBL (Geyer and Stutz, 2004a; Stutz et al., 2004b). As a consequence of the vertical profiles of O_3, NO_3 and N_2O_5, the loss of VOCs through direct oxidation and loss of NO_x through surface uptake of N_2O_5 become altitude dependent as well. A 1-D chemical transport model study reproduced the general features of these vertical profiles observed in field campaigns. The study also pointed out that N_2O_5 vertical transport plays an important role for the radical chemistry at night (Geyer and Stutz, 2004a; Stutz et al., 2004b).

These studies clearly show that chemistry in the stable NBL is height dependent. Vertical profiles of trace gases and their chemistry are complex and dependent upon meteorological conditions. As a consequence, measurements of trace gases at single altitudes are not representative for the entire NBL. The lifetime and the budget of reactive species cannot be simply derived from single-altitude measurements alone. In addition, high levels of O_3 and NO_3 in the upper NBL lead to chemical processes that occur aloft well before they are present at the surface during morning hours. This effect is not well considered in current measurement strategies. Therefore, comprehensive observations of boundary layer vertical distributions of both reactive species and meteorological parameters during night-time and even morning hours are required for a better understanding of the height-dependent nocturnal chemistry system and the consequent influence on daytime chemistry.

However, very few studies on this topic have been made thus far, and most of them were carried out in suburban or rural areas. The height-dependent nocturnal chemistry in urban areas with strong surface emissions has been paid surprisingly little attention. Large uncertainties greatly limit our ability to qualitatively and quantitatively describe the complex interaction of chemistry with meteorology in a heavily polluted NBL. For example, the removal of O_3 as well as its precursors, VOCs and NO_x, involves various height-dependent chemical processes, which are currently only known based on surface measurements. Night-time surface emissions in strongly polluted areas can result in surface

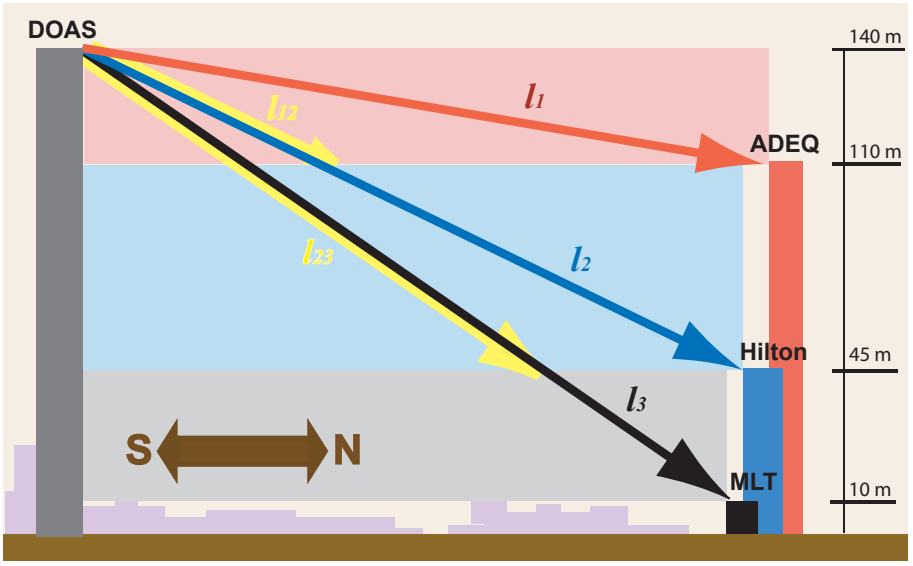

Fig. 1. Schematics of the DOAS light paths in Phoenix. The figure also shows the height intervals for which average concentrations were retrieved. The parameters in the figures are explained in detail in Sect. 2.2 and Table 1. The red rectangle refers to the upper box, blue refers to middle box and gray refers to lower box.

accumulation of O_3 precursors. The budgets of both O_3 and its precursors in the NBL and the ultimate influence of the height-dependent system of emissions, chemistry, and vertical transport in the NBL on daytime O_3 levels are not clear. As predicted by a recent chemical transport model study by our group (Geyer et al., 2003; Geyer and Stutz, 2004a), high surface NO emissions in urban areas are expected to influence both the vertical profiles and budgets of the core species of nocturnal chemistry such as O_3, NO_2, NO_3 and N_2O_5. In order to provide field data to test the predictions as well as to study the budget of various nocturnal trace gases in polluted urban areas, vertical distributions of a series of trace species as well as meteorological parameters were measured simultaneously during a field campaign in downtown Phoenix in summer 2001. Here we present these observations and discuss the vertical variations of the related chemical processes and the implications for O_3–NO_x system in the stable NBL.

2 Experimental section

In June 2001, a field experiment funded by the U.S. Department of Energy was conducted in the downtown area of Phoenix, AZ. Measurements were made at various locations in the city including the roofs of several high-rise buildings. UCLA's long-path Differential Optical Absorption Spectroscopy (DOAS) system was operated to provide 24-h continuous measurements of vertical distributions of a number of trace species in the open atmosphere. Meteorological parameters such as relative humidity (*RH*), wind direction and speed were monitored at various fixed altitudes. Potential temperature profiles were measured using balloon sondes. In addition, in situ measurements of NO were made at different altitudes. This section provides details of the instrumental setup and the data analysis.

2.1 DOAS measurements

DOAS is a technique that identifies and quantifies trace gases by their distinctive UV-visible narrow band absorption structures in the open atmosphere (Platt, 1994). The main advantage of DOAS is the absolute quantification of species at low concentrations without disturbing the composition of the observed air mass. The quantification is solely based on the measured optical density and the known absorption cross sections of the detected species. In addition, the absence of sampling problems and the insensitivity of its accuracy to the presence of aerosols make this technique ideal for observations in the polluted atmosphere.

During this two-week field experiment (16 June 2001–1 July 2001), the UCLA long path DOAS instrument was set up on the 39th floor of BankOne, the highest building in downtown Phoenix, about 140 m above the ground level (Figs. 1 and 2). Details of the instrument can be found in Alicke et al. (2002). In short, light from a 500 W Xe-arc lamp was fed into a 1.5 m double Newtonian telescope, which was used to send a highly collimated light beam into the open atmosphere and to collect the light reflected back by arrays of quartz cube-corner prisms (retroreflectors). Three retroreflector arrays were mounted on the roofs of separate buildings (ADEQ, Hilton, and MLT) at a distance about 3.3 km north of BankOne (see Fig. 1). The altitudes and lengths of these three light paths are listed in Table 1. The average trace

Table 1. Light paths and building heights at Phoenix site.

Instrument Setup	Height (m)		Light Path	
			Height (m)	Length (km)
DOAS telescope on BankOne	~140			
Upper Retro on ADEQ	~110	Upper	110~140	l_1=3.51×2
Middle Retro on Hilton	~45	Middle	45~140	l_2=3.29×2
Lower Retro on MLT	~10	Lower	10~140	l_3=3.23×2

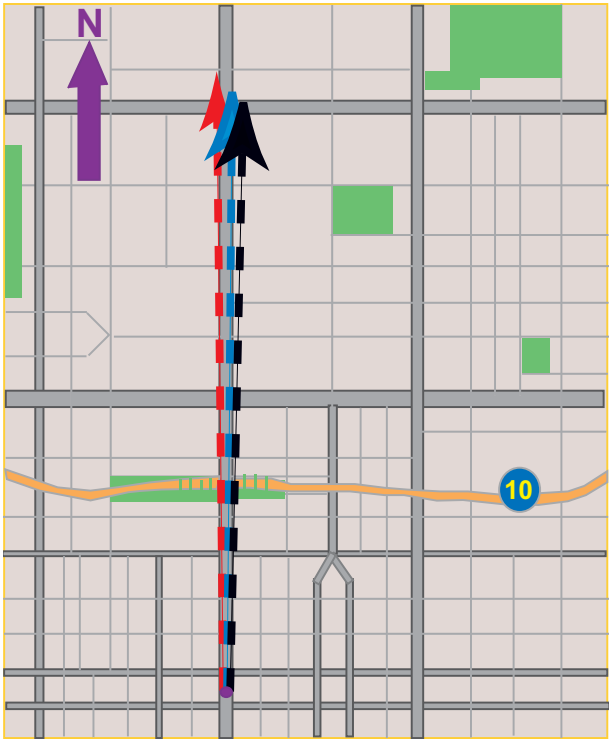

Fig. 2. Map illustration of the DOAS light paths in downtown Phoenix. The lengths of the light paths are given in Table 1. The color coding of the paths is according to Fig. 1.

gas concentrations along each light path were monitored by sequentially aiming the telescope at the three retroreflector arrays. The duration of a typical measurement cycle covering all three light paths was about 15–20 min depending on the atmospheric visibility.

Figures 1 and 2 illustrate that the light paths were superimposed in the horizontal but separated in the vertical direction. The paths ran along one direction of the street grid which connnects the downtown and northern uptown regions of Phoenix. Because traffic was, to a large extent, spatially homogeneous in downtown Phoenix, the chance of inhomogeneities of trace gas distributions in the horizontal direction was expected to be small, particularly considering that the DOAS measurement averaged over 3.3 km. The in situ data of wind profiles at different altitudes provide additional helpful information for the possible influence of horizontal inhomogeneity (see Sect. 2.3). The buildings and structures along the light paths were mostly low (1–3 stories) except for the areas at the two ends of the paths. The area between downtown and uptown Phoenix therefore offers an ideal location for our measurements, since the impact of street canyons was expected to be small.

2.2 Data analysis

NO_2, HONO, HCHO and O_3 were measured in the near UV spectral region according to their distinctive absorption structure in the wavelength range of 300–380 nm. NO_3 was detected separately at higher wavelengths (610–680 nm). The detailed spectra analysis procedures for the two spectral regions are described in Alicke et al. (2002), Geyer et al. (1999). Table 2 lists the spectral windows used for the analysis and the references for the literature absorption cross sections used in the analysis.

In order to study the vertical distribution of pollutants, the concentration results along light paths derived by the DOAS analysis need to be converted into concentrations averaged over distinct height intervals. The first step in this deconvolution process is to solve the temporal problem introduced by the sequential measurement. To account for the temporal variation during a measurement sequence, a linear function was used to interpolate the upper and middle light path data to the time of the lower light path measurements. The concentration at time t was derived with the concentrations at t_1 (before t) and t_2 (after t):

$$C_t = C_{t1} + \frac{C_{t2} - C_{t1}}{t_2 - t_1} \cdot (t - t_1)$$

Here we assumed that during the short time period between scans (at most ~35 min), the change of trace gas concentrations can be approximated by a linear function. The results from measurement cycles longer than 35 min were filtered out in the calculation. While this is generally a good approximation for long-path data, during periods with rapid concentration changes this approach may lead to inaccurate results. However, these time periods can be easily identified based on the original data and excluded.

The trace gas concentrations averaged over three height intervals (C_{up}, C_{mid}, and C_{low}) were then derived using the

Table 2. Detection limits for each measured trace gas.

Species	Fitting window (nm)	Literature of absorption cross sections	Average Detection Limit (2σ) Upper box (110–140 m)	Middle box (45–110 m)	Lower box (10–45 m)
NO_2	336∼371	Voigt et al. (2002)	0.11 ppb	0.18 ppb	0.64 ppb
HONO	336∼371	Stutz et al. (2000)	0.04 ppb	0.07 ppb	0.25 ppb
HCHO	303∼326	Meller and Moortgart (2000)	0.23 ppb	0.38 ppb	1.4 ppb
O_3	303∼326	Bass and Paur (1984)	1.7 ppb	2.8 ppb	10 ppb
NO_3	617∼668	Sander (1986)	3.5 ppt	6.0 ppt	18 ppt

following equations based on concentrations averaged along each light path (C_1, C_2, and C_3).

$$C_{\mathrm{up}} = C_1$$

$$C_{\mathrm{mid}} = \frac{C_2 \cdot l_2 - C_1 \cdot l_{12}}{l_2 - l_{12}}$$

$$C_{\mathrm{low}} = \frac{C_3 \cdot l_3 - C_2 \cdot l_{23}}{l_3 - l_{23}}$$

The length variables l_2, l_3, l_{12}, and l_{23} are defined in Fig. 1. C_{up}, C_{mid}, and C_{low} are not only averaged in the vertical, but also in the horizontal direction. Figure 1 illustrates the three boxes of air mass over which the averaging occurs. For the remainder of this paper, we assume that the differences in C_{up}, C_{mid}, and C_{low} are dominated by the vertical variations in the concentrations. The validity of using multi-angle long path DOAS measurements to estimate vertical profiles was discussed in detail in (Stutz et al., 2002, 2004b) and is not repeated here.

Due to the error propagation through the calculation and the difference in light path lengths, C_{low} generally has larger errors and higher detection limits than C_{up} and C_{mid}. The mean detection limits in all height intervals for each measured species are listed in Table 2. All errors are reported as one standard deviation σ (Stutz and Platt, 1996). The reported detection limits are twice the errors.

Based on these results, the overall vertical gradients of trace gas concentrations between 27.5 m and 125 m altitude can be estimated with a linear approximation,

$$\frac{\Delta C}{\Delta \mathrm{z}} = \frac{C_{\mathrm{up}} - C_{\mathrm{low}}}{\mathrm{z_{up}} - \mathrm{z_{low}}}$$

where $\mathrm{z_{up}}$ and $\mathrm{z_{low}}$ refer to the central height of the upper and lower box respectively (i.e., 125 m and 27.5 m). Our earlier studies show that the vertical trace gas profiles in the NBL show complex non-linear shapes. The gradient calculated in this equation is thus only used as a qualitative approach to illustrate the general features of our measured time series, rather than a quantitative description of the profiles. Since the trace gas concentrations resulted from spectra fitting and the above-mentioned derivation procedure, negative values may appear when the actual concentrations were below DOAS detection limits, especially for the lowest height interval. To estimate the vertical gradient with real physical meaning, the negative concentration values were set to zero when calculating ($C_{\mathrm{up}}-C_{\mathrm{low}}$).

2.3 In situ measurements

Meteorological parameters such as *RH*, temperature, wind speed and direction were continuously monitored close to the retroreflectors on top of the buildings with Campbell Scientific Inc. weather stations. Since the observation of vertical profiles with the long path DOAS technique is based on the assumption that there is no influence from horizontal advection at different altitudes, the wind profiles measured at different altitudes provide a useful reference to exclude cases when inhomogeneities in the horizontal advection contribute to the gradients (Fast et al., 2005). Potential temperature profiles which indicate the NBL stability and height were also provided by balloon soundings during selected nights. The balloons were launched from the Vehicle Emission Laboratory, 7 km east of BankOne (Doran et al., 2003). On the 39th and 16th floor of the BankOne building, NO and CO mixing ratios were measured by chemiluminescence (Thermo Environmental 42S) and gas filter correlation IR, which helps evaluate the relative emission strength at the surface (Doran et al., 2003). A ground-based air quality monitoring station of Arizona Department of Environmental Quality monitored continuously the main meteorological parameters and mixing ratios of air pollutants such as CO, NO_x and O_3 at ground level in central Phoenix, approximately 3 km from BankOne, in a southwesterly direction. The photolysis rate of NO_2 (J_{NO2}), an indicator of the solar radiation strength, was monitored by a filterradiometer (Meteoconsult) at the Vehicle Emission Laboratory.

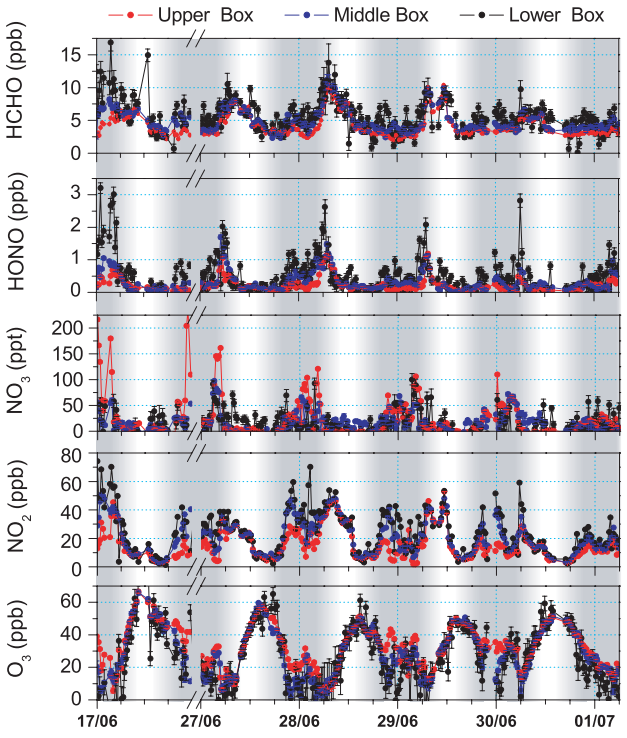

Fig. 3. Overview of the vertical profiles of measured trace species during 17 June–1 July 2001 in Phoenix. The background is shaded to draw attention to the nocturnal data. Gray and white denote nighttime and daytime, respectively. The transition between the colors shows sunrise and sunset periods. Lines in different colors shows the time series of average trace gas mixing ratios at different height intervals (see Fig. 1 and Table 2 for details of the height intervals). We will use the same color coding for all the following figures. The length of the error bars is one standard deviation.

3 Measurement results

3.1 Overview of vertical variations of measured species

An overview of the measured vertical profiles of trace gases is shown in Fig. 3. In general, clear vertical variations of trace gas levels in the three height intervals were observed during most nights in this experiment. O_3 mixing ratios in downtown Phoenix showed diurnal variations typical for polluted urban areas, with daytime maxima of up to 70 ppb and completely depleted O_3 on some nights. This variation is reversed in the NO_2 time series, which showed low NO_2 levels below 10 ppb during the day and maxima of up to 70 ppb at night. During all the nights shown in Fig. 3, strong vertical variations of NO_2 and O_3 mixing ratios were observed. The negative NO_2 gradient and positive O_3 gradient agree well with earlier observations in various rural and suburban areas (Glaser et al., 2003; Pisano et al., 1997; Stutz et al., 2004b), but with significantly larger magnitudes due to the higher emission rates in downtown Phoenix. The gradients were sustained until the morning hours and then gradually disappeared after the onset of convective mixing.

NO_3, which is formed by the reaction of NO_2 with O_3 and removed mainly by its reaction with ground-level emitted NO_x and VOCs, also developed strong positive vertical gradients during most nights. The magnitude of both NO_3 mixing ratios and vertical gradients depends on the levels of NO_2 and O_3. During the night of 30 June–1 July, for example, NO_2 levels were relatively low, indicating a weaker NO_x emission strength compared with other nights. Accordingly, NO_3 levels were only slightly above the detection limits due to the low production rate and showed little gradient as a result of the low NO emission from the surface. This behavior is in agreement with the results of (Geyer and Stutz, 2004a; Hov, 1983). It should be noted that surprisingly high NO_3 levels were observed in Phoenix, with nocturnal maxima between 50–200 ppt. While the cause of this high NO_3 will be discussed further below, it is worth pointing out that the unique meteorological conditions in Phoenix could play a role. Daytime temperatures reached above 40°C and cooled down to minima of 25–30°C at night. The *RH* was below 20% during the day and below 40% during the night, except for 26 June when *RH* reached 70%. Both high temperatures and low *RH* are favorable for the development of high NO_3 levels due to the decreased importance of N_2O_5 and its surface uptake (Geyer and Stutz, 2004a; Hov, 1983).

HONO, which is directly emitted from traffic and chemically formed in the atmosphere mainly by the heterogeneous hydrolysis of NO_2 on various surfaces (Finlayson-Pitts et al., 2003; Stutz et al., 2004a), showed negative vertical gradients. Because the gradients are of the same sign as those of NO_2, it is difficult to discriminate between the different sources of HONO. However, the negative gradients of HONO together with its gradual accumulation during night, with the highest HONO levels in the later part of the night, point to a formation close to the surface. In some cases, the HONO gradients persisted a few hours after sunrise when photolysis production of OH started. Since HONO is an important OH source in the morning, leading to a significant increase of O_3 concentrations in the polluted boundary layer (Alicke et al., 2002; Aumont et al., 2003), the vertical gradient of HONO and its implications will be investigated further in an upcoming publication.

Significant negative vertical gradients of HCHO up to 0.12 ppb/m were observed during the night in Phoenix (for example the early morning of 17 June in Fig. 3). Since the photochemical production pathways of HCHO are absent at night, this strong HCHO profile implies the existence of another significant source, which should be active close to the ground. In earlier traffic tunnel measurements, significant amounts of primary HCHO from auto exhaust were observed (Kurtenbach et al., 2002). The night-time traffic in downtown Phoenix could therefore be a major emission source for HCHO. Although we have little information on the emission ratio of HCHO/NO_x in the vehicle exhaust and the other

possible sources responsible for the high night-time HCHO emission in Phoenix, it can be concluded based on the observations that photochemistry is not the only major source for atmospheric HCHO. Future studies, for example tunnel measurements of emission ratios of HCHO, are suggested to quantify the contribution of direct emissions to the nocturnal atmospheric HCHO in urban areas.

The observed general patterns of trace gas vertical profiles in the NBL agree well with earlier modeling studies for typical urban cases (Geyer and Stutz, 2004a). According to the model results, the shape of these vertical profiles depend predominantly on the nocturnal atmospheric stability and the surface emission rates of NO and VOCs. To validate these model predictions, we have selected two nights illustrating the impact of these factors on the NBL in Phoenix.

3.2 A case with strong surface emissions and high stability

The night of 16 June–17 June (Fig. 4) was one of the most polluted during the experiment. Levels of CO measured at ∼50 m altitude at BankOne were above 1 ppm around midnight (not shown here). During most other nights, CO levels were high only during morning rush hour, which was absent on 17 June (Sunday). We attribute the unusually high CO levels on this weekend night to the heavy traffic caused by an event that occurred in the stadiums near downtown Phoenix. The strong emissions are also reflected by the in situ data of NO at BankOne, which will be further discussed in Sect. 4.1.

A strong temperature inversion and low wind speeds, indicated by the in situ meteorological data (Fig. 5), show that this night was also characterized by a high vertical stability of the NBL. The temperature difference between Hilton (∼45 m) and ADEQ (∼110 m) was about 3–5 K during most parts of the night, especially before 04:00. Wind speeds rarely reached above 2 m/s during this period. *RH* was as low as 5–20%. Potential temperature profiles by balloon soundings (Fig. 6) further demonstrate the surface inversion strength and the approximate height of the stable NBL. Both balloon soundings and in situ measurements show a decrease of the temperature inversion as the night proceeded, in particular after 04:00.

Due to the strong surface emissions and the high stability of the NBL, clear positive vertical gradients of O_3 and NO_3 and negative gradients of NO_2, HONO and HCHO were observed throughout this night. The vertical profiles were particularly strong before 04:00. The high NO_2 levels of up to 80 ppb in the lower box during this period are in agreement with strong night-time NO_x emissions and the conversion of NO into NO_2 through the reaction with O_3. As a result, O_3 mixing ratios in the lower box ranged from below detection limits to at most 20 ppb, implying a surface O_3 depletion as reported in the earlier studies (Colbeck and Harrison, 1985; Cros et al., 1992; Gusten et al., 1998). Because the vertical mixing was greatly limited, smaller concentrations of NO_2 and larger concentrations of O_3 were expected at higher altitudes, especially above the nocturnal inversion height. The potential temperature profile at midnight (Fig. 6) reveals that the strong surface inversion led to a stable NBL with a height of less than 100 m. The upper box, above the inversion height, was left in the RL and thus largely decoupled from the ground emissions. Consequently, trace gas mixing ratios in the upper box reflected the composition of the RL and were close to those during daytime. As shown in Fig. 4, the upper box O_3 levels were significantly higher than those of the lower and middle boxes with a maximum of over 50 ppb, resulting in a strong positive O_3 gradient of up to 0.4 ppb/m. NO_2 mixing ratios in the upper layer were in the range of 5–20 ppb, leading to negative NO_2 gradients as large as −0.6 ppb/m. The fact that the O_3 and NO_2 gradients have similar magnitudes but opposite signs will be discussed further below (see Sect. 4.2). For the other important night-time oxidant, NO_3, surprisingly high levels over 200 ppt were observed in the upper box. The lower box NO_3 levels rarely reached above 50 ppt, leading to maximum NO_3 gradients of 2 ppt/m. As a consequence of the vertical profiles of both O_3 and NO_3, a strong vertical variation of the atmospheric oxidation capacity within and above the NBL is expected. According to the studies of Geyer and Stutz (2004a, b), the stable NBL at midnight in an urban case with strong emissions can be subdivided into an unreactive ground layer, an unreactive upper layer above ∼80 m and a reactive mixing layer centered around 50 m altitude. Our observations during this night agree well with those model study results.

From 04:00 to sunrise at about 05:30 (see photolysis rate (J_{NO2}) in Fig. 5), the vertical gradients were significantly reduced. The smaller temperature inversion and the higher wind speeds indicate a weaker stability. This early morning transition was described by Doran et al. (2003), who speculated that large scale convergence and resulting upward motions over the Phoenix valley was the cause for the increase in vertical mixing prior to sunrise.

After sunrise, radiative heating results in a quick breakup of the surface inversion. A well-mixed layer starts to grow upward from the surface. In this case, the convective layer grew up to ∼100 m at 06:00. By 08:00, a typical convective boundary layer with a depth of a few hundred meters had developed. Consistent with this morning transition, the observed vertical variations in Fig. 4 started to regress after 05:00 and had disappeared completely by 08:00 due to the strong vertical mixing. In addition, as a result of the increasing photolysis, NO_2 and HONO levels decreased while O_3 was produced by photochemistry and its mixing ratios increased at all altitudes.

3.3 A case with weaker surface emissions and varying stability

The night of 26 June–27 June (Fig. 7), a typical weekday night, was characterized by relatively weaker surface emissions and different vertical stabilities than the previous case.

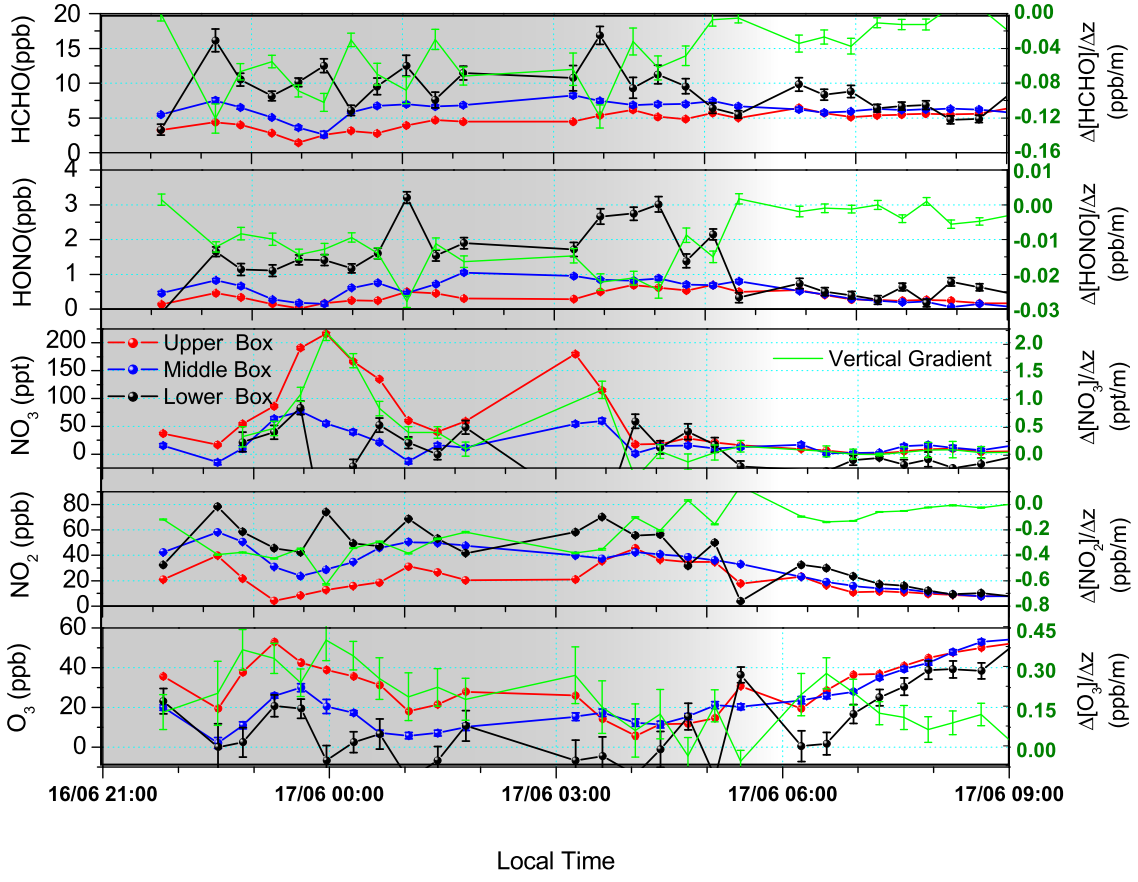

Fig. 4. Vertical profiles of trace gas distribution on the night of 16 June–17 June 2001. The left axis refers to the box-averaged mixing ratios. The right axis refers to the vertical gradients (green color) calculated based on the upper and lower box data.

CO mixing ratios were around 250 ppb until the onset of the morning rush hour, when they reached a maximum of near 800 ppb. Though the CO levels are also influenced by vertical transport, the predominant cause for the lower nocturnal CO levels than those of the night of 16 June–17 June, which included an evening event with high traffic levels, is the lighter traffic during typical weeknights in Phoenix. In addition, the measured temperature profiles and wind speeds on top of ADEQ generally show that this night showed weaker stability than 16 June–17 June (see Fig. 8). Accordingly, the observed trace gas vertical gradients on this night were clearly smaller than those of the high emission and high stability case.

The in situ meteorological data also illustrate two periods during this night with considerably different atmospheric stabilities (highlighted in Fig. 8): 1) A relatively unstable period with high wind speed around 4 m/s and no detectable temperature inversion from about 23:00 to 01:00. 2) A very stable period with very weak wind and a clear temperature inversion from 03:00 until 05:00. Because the difference in local emissions during the two periods is expected to have less impact (according to the in situ CO data), the difference in vertical variations between these two selected periods was most likely caused by the different NBL stabilities. During the first highlighted period, the strong wind induced effective vertical mixing in the NBL, leading to negligible temperature gradients (Fig. 8). Consistent with the meteorological observations, the vertical trace gas gradients in Fig. 7 were undetectable or close to zero in these two hours. In addition, NO_3 levels were found to be close to zero during this time, most likely due to the efficient transport of surface emitted NO into higher altitudes where it destroyed NO_3. This will be further discussed with calculated NO_3 production rate and steady state lifetime of NO_3 in Sect. 4.3. During the second period, wind speeds decreased to below 1 m/s and a clear temperature inversion developed (Fig. 8). Vertical mixing during this calm period was thus suppressed. Consequently the measured trace gas vertical gradients became stronger, reaching the maxima after 04:00 (Fig. 7). O_3 levels in the lower box rapidly decreased from ~20 ppb to zero through the reaction with surface emitted NO, while the levels in the middle and upper boxes remained approximately constant. Similarly, NO_2, HCHO, and HONO mixing ratios in the lower box increased, while the levels in the other two boxes

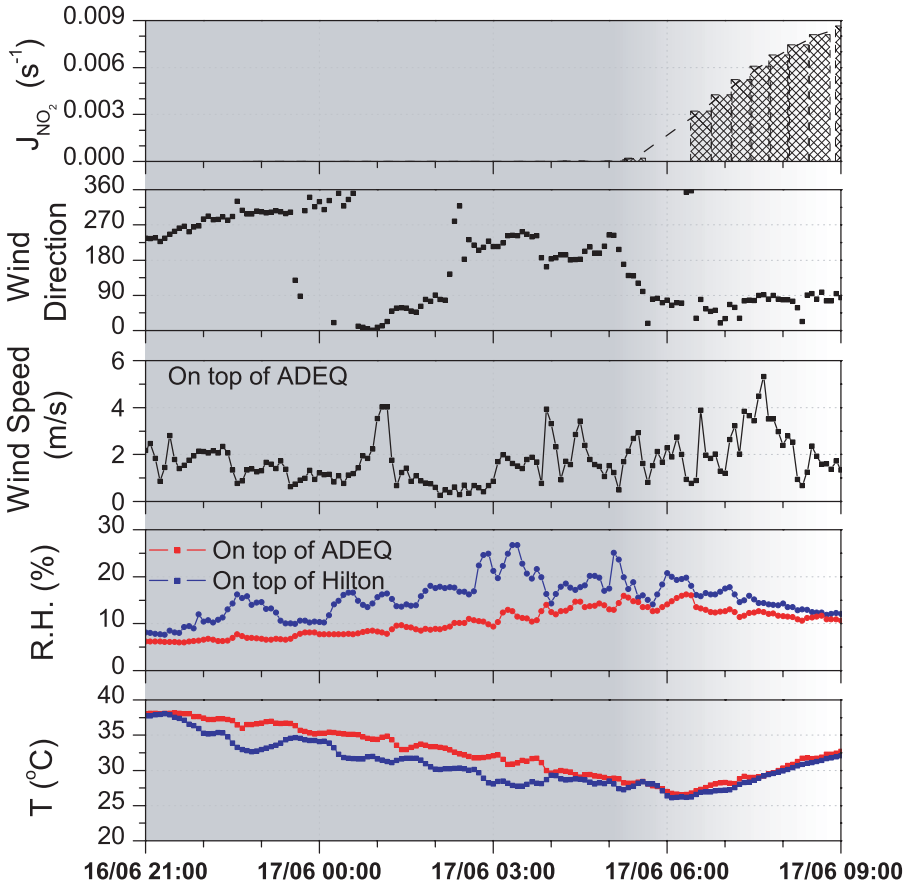

Fig. 5. Meteorological conditions on the night of 16 June–17 June 2001. ADEQ measurements were made at ~110 m above the ground. Hilton data were taken at ~45 m above the ground. For wind direction, north is 0 and east is 90 degree. The time series of the NO_2 photolysis frequency, J_{NO2}, is included to show the time of sunrise.

had little change. With little NO being transported upward, the NO_3 level in the upper box increased rapidly and a maximum of ~150 ppt was observed. After 05:00, an increase in wind speed again reduced the atmospheric stability and the vertical gradients of trace gases. Similar to the previous case, the vertical profiles disappeared completely after 08:00 when a typical convective boundary layer was established. The short term negative vertical gradients of NO_2, HONO and HCHO about 1 h after sunrise reflect the weekday morning rush hour. Therefore, the behaviors of vertical gradients and the NBL stability during these two periods clearly show the influence of vertical mixing on the trace gas profiles.

Table 3. Key chemical reactions influencing the levels of O_3, NO_2 and O_x in the NBL.

(R1)	$NO + O_3 \rightarrow NO_2 + O_2$
(R2)	$NO_2 + O_3 \rightarrow NO_3 + O_2$
(R3)	$NO_3 + NO \rightarrow NO_2 + NO_2$
(R4)	$NO_3 + VOCs \rightarrow \ldots\ldots \rightarrow$ organic nitrate + other products
(R5)	$NO_3 + NO_2 + M \leftrightarrow N_2O_5 + M$
(R6)	$N_2O_5 + H_2O \xrightarrow{\text{aerosols}} 2HNO_3$

4 Discussion

Our observations of vertical trace gas profiles offer the unique opportunity to study the vertical variations of nocturnal chemistry as well as the budgets of O_3 and NO_2. In this section, we will concentrate on the analysis of the budget of the O_3-NO_x system based on the observations. A detailed study of the chemical pathways in the NBL and the impact of vertical mixing by a chemical transport model will be presented in a forthcoming publication. The following section will give a brief review of the processes dominating the budgets of O_3, NO_2, and thus O_x (the sum of O_3 and NO_2) that will be used in the discussions. The involved key chemical reactions are summarized in Table 3.

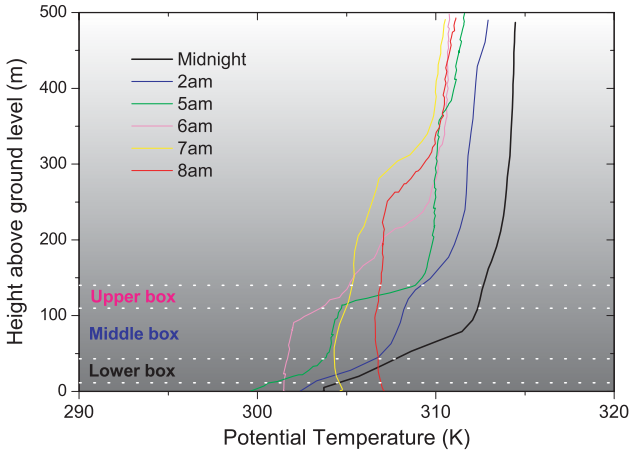

Fig. 6. Potential temperature profiles in the lower atmosphere on the night of 16 June–17 June 2001. The change of the strength and the depth of the potential temperature inversion with time illustrates the development of the stable NBL during the night and the growth of the convective boundary layer after sunrise.

4.1 Nocturnal processes influencing O_3, NO_2, and O_x levels

Due to the absence of sunlight, O_3 undergoes pure loss in the NBL. The dominant chemical sink of O_3 in urban areas with strong surface emissions is its rapid reaction with freshly emitted NO, a process known as NO titration (R1 in Table 3). However, this transformation of O_3 to NO_2 only temporarily removes O_3 from the boundary layer, since the photolysis of NO_2 during the next morning will lead to a re-release of O_3. The photostationary state between NO, NO_2 and O_3 can be used to illustrate the impact of nocturnal NO emissions on the morning O_3 budget. The distribution between NO_2 and O_3 during the morning hours, ignoring photochemical chain production of O_3, can be described by the Leighton ratio $[O_3]=\frac{J_{NO2}}{k_1}\cdot\frac{[NO_2]}{[NO]}$ (Finlayson-Pitts and Pitts, 2000), which includes a dependence on the photolysis rate of NO_2. The sum of O_3 and NO_2, O_x, will remain constant, assuming the absence of O_3 or NO_2 loss processes other than (R1) and NO_2 photolysis. Based on the Leighton ratio, one can derive an expression for the steady state O_3 concentration before sunset and after sunrise, which depends on the levels of O_x, NO_x ($NO+NO_2$), and J_{NO2}:

$$[O_3]=\frac{1}{2}\left([O_x]-[NO_x]-\frac{J_{NO2}}{k_1}+\sqrt{\left([NO_x]-[O_x]+\frac{J_{NO2}}{k_1}\right)^2+4\frac{J_{NO2}}{k_1}[O_x]}\right) \quad (1)$$

To determine the influence of nocturnal NO emissions, we start with the initial NO_x concentrations at sunset, $[NO_x]_{ss}$. The sunrise NO_x is thus defined by $[NO_x]_{sr}=[NO_x]_{ss}+E_{NO}$, where E_{NO} represents the total emissions of NO throughout the night. The difference between O_3 levels at sunset and the next sunrise, $[O_3]_{sr}-[O_3]_{ss}$, shows the effective O_3 destruction due to nocturnal NO emissions assuming that J_{NO2} is equal in both cases. An O_3 destruction efficiency of NO emissions is defined as:

$$D_{O3}=-\frac{\Delta[O_3]}{\Delta[NO_x]}=\frac{[O_3]_{ss}-[O_3]_{sr}}{E_{NO}}.$$

The change in $[O_3]$ due to the increasing $[NO_x]$ (i.e., $-D_{O3}$) can be approximately expressed by the first order differentiation of Eq. (1):

$$\frac{\partial[O_3]}{\partial[NO_x]}=\frac{1}{2}\cdot\left(\frac{[NO_x]-[O_x]+\frac{J_{NO2}}{k_1}}{\sqrt{([NO_x]-[O_x]+\frac{J_{NO2}}{k_1})^2+4[O_x]\cdot\frac{J_{NO2}}{k_1}}}-1\right)<0 \quad (2)$$

Though the value of D_{O3} calculated with the above approximation depends on different combinations of $[O_x]$, $[NO_x]$, E_{NO}, and J_{NO2}, it should be noted that the expression of Eq. (2) is always smaller than zero. The nocturnal emission of NO should thus always lead to lower O_3 levels at sunrise than those before the previous sunset in all cases (i.e., $D_{O3}>0$).

The second order differentiation of Eq. (1), $\frac{\partial^2[O_3]}{\partial[NO_x]^2}\approx\frac{\partial(-D_{O3})}{\partial[NO_x]}$, is positive. This further demonstrates that the O_3 destruction efficiency, D_{O3}, decreases with increasing NO_x levels. Here we can discuss an example with $[O_x]$=60 ppb and J_{NO2}=0.005 s^{-1}. At low $[NO_x]_{ss}$ levels (<10 ppb) and low to moderate E_{NO}, D_{O3} is found in the range of 0.7–0.9. At high levels of $[NO_x]_{ss}$(40 ppb), D_{O3} decreases to 0.4–0.5. Similarly, the magnitude of D_{O3} is also found to decrease with increasing E_{NO}. Therefore, the impact of nocturnal NO emissions on the O_3 budget depends on various parameters and needs to be determined for every case separately. However, it is clear that (R1) does ultimately destroy O_3, considering the difference in O_3 levels before sunset and after sunrise.

In addition to (R1), other processes influence the concentrations of O_3 and NO_2 in the NBL and change the total O_x level directly. One may assume that the loss of one O_x during night-time leads to exactly a loss of one O_3 in the next morning. However, Eq. (3) illustrates that, considering the effect of Leighton ratio Eq. (1), the reduction of O_3 is less than one.

$$\frac{\partial[O_3]}{\partial[O_x]}=\frac{1}{2}\cdot\left(\frac{[O_x]-[NO_x]+\frac{J_{NO2}}{k_1}}{\sqrt{([NO_x]-[O_x]+\frac{J_{NO2}}{k_1})^2+4[O_x]\cdot\frac{J_{NO2}}{k_1}}}+1\right)<1 \quad (3)$$

In the following, we will distinguish the above-discussed process, which converts O_3 into NO_2 without changing O_x levels and influences the O_3 budget indirectly, from those that change the total O_x and influence the O_3 budget directly.

The further oxidation of NO_2 forms NO_3 (R2) and temporarily destroys one O_3 and one NO_2, i.e., two O_x molecules. However, in urban areas the fast reaction of NO_3 with ground-level emitted NO is the major sink of NO_3, and

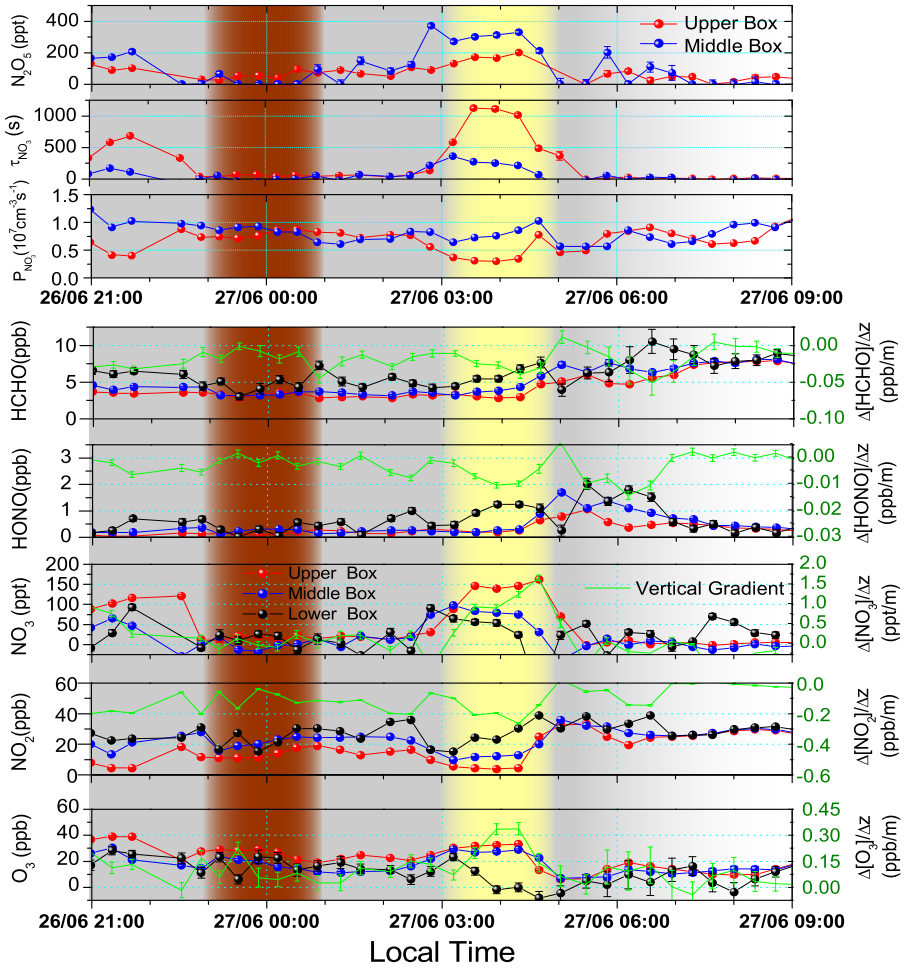

Fig. 7. Vertical profiles of trace gas distribution on the night of 26 June–27 June 2001. The lower panels illustrate the measured trace gas mixing ratios at three different height intervals and the calculated vertical gradients. The upper panels show the calculated NO_3 production rate P_{NO3}, NO_3 chemical steady-state lifetime τ_{NO3}, and the steady-state N_2O_5 levels in the upper and middle height intervals.

reforms two O_x (R3). The total O_x is thus conserved in the reaction system of (R2) and (R3) in the NBL, acting similarly to (R1) by converting O_3 into NO_2. Therefore, only the transformations of NO_3 that do not regenerate O_x can be considered a final loss of O_x.

As one of the dominant oxidants in the NBL, NO_3 oxidizes various VOCs forming organic nitrates (R4). Although the further reactions of some organic nitrates can produce NO_2, the majority of these reactions do not regenerate O_x and thus lead to the ultimate O_x loss (Stockwell et al., 1997). In addition, the reaction of NO_3 with NO_2 results in the formation of an important reservoir species, N_2O_5, through (R5). The uptake of N_2O_5 on aerosols (R6) is an indirect sink for NO_3 and another loss process of O_x. (R5) also consumes an additional O_x in the form of NO_2. It has to be noted that the efficiency of (R5) is strongly dependent on the ambient *RH*, which will be discussed further below.

The direct oxidation of VOCs by O_3 is slow compared to other O_x loss processes and has little significance for the O_x budget in urban areas.

Dry deposition of both NO_2 and O_3 on the ground and direct uptake on aerosols also lead to O_x loss. The description of dry deposition in the urban NBL is challenging due to the poorly quantified vertical exchange rates and the simultaneously acting chemistry. Air quality models often employ a formalism describing deposition flux (j_{dep}) by the product of a deposition velocity (v_{dep}) at one altitude and the concentration of the trace gas (C): $j_{dep}=v_{dep}\times C$. This formalism is often inaccurate for O_3 and NO_2 in urban areas due to the simultaneously acting chemical transformation of O_3 into NO_2 (R1) (Geyer and Stutz, 2004a; Hov, 1983).

Vertical transport of O_3 into and of NO_2 out of the NBL is a source and a sink of these gases in the NBL. We will discuss below how this process influences O_x levels.

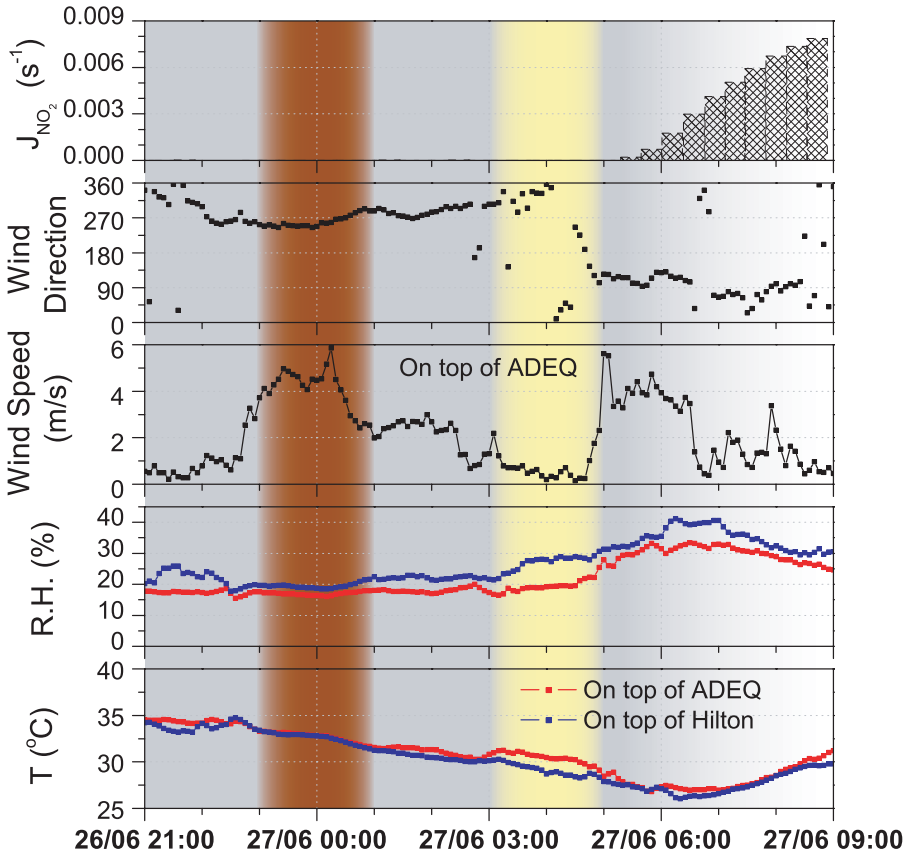

Fig. 8. Meteorological conditions on the night of 26 June–27 June 2001 (see caption of Fig. 5 for an explanation of the ADEQ and Hilton data). The brown bar indicates a period of low stability, while the yellow bar shows a period of strong stability.

Finally one also has to consider the direct emission of NO_2 through combustion processes. Since the emission ratio of NO_2/NO_x is typically less than 10%, the impact of direct emissions to the total O_x budget in the NBL is, in most cases, small. However, it will be shown later that under some circumstances the influence of NO_2 emissions can be observed.

Based on the above discussions, it is clear that the analysis of the nocturnal O_3, NO_2, and O_x budgets requires the separation of various processes that influence this system. In particular, processes that change O_3 and NO_2 levels without changing the level of O_x need to be treated separately. Consequently, we will have a closer look at the NO titration process and the O_3-NO_2-O_x system in Phoenix in Sect. 4.2. The contribution of NO_3 and N_2O_5 chemistry, which plays an important role in the nocturnal O_x loss and the ultimate O_3 removal, will be discussed in Sects. 4.3 and 4.4. Finally, a semi-quantitative calculation of the O_3, NO_2 and O_x budgets will be given in Sect. 4.5.

4.2 The role of NO titration in the NBL chemistry

The first step to analyze the processes determining the NBL O_3 budget is the investigation of the role of reaction (R1). The altitude dependence of nocturnal chemistry is controlled by the NO emission rate, in addition to the vertical stability of the NBL (Geyer and Stutz 2004a; and Hov, 1983). As shown in Sect. 3, night-time NO emissions followed by the fast NO titration led to positive O_3 vertical gradients and negative NO_2 gradients of similar magnitudes in Phoenix. It is thus interesting to discuss the vertical profiles of total O_x in the NBL. Here, three different scenarios of observed nocturnal vertical profiles in Phoenix are discussed.

4.2.1 The uniform O_x vertical profile in a typical urban case in Phoenix

In a typical case in Phoenix, for example the night of 28 June–29 June 2001 (Fig. 9), clear vertical variations of O_3 and NO_2 levels were observed throughout the night until the onset of a strong morning vertical mixing, which agrees well with earlier observations (Aneja et al., 2000; Colbeck and Harrison, 1985; Glaser et al., 2003; Gusten et al., 1998; Zhang and Rao, 1999) and model simulations (Geyer and Stutz, 2004a; Hov, 1983). The O_3 and NO_2 gradients show a remarkable anti-correlation even during rapid variations (marked by the yellow arrows in Fig. 9). In contrast, the

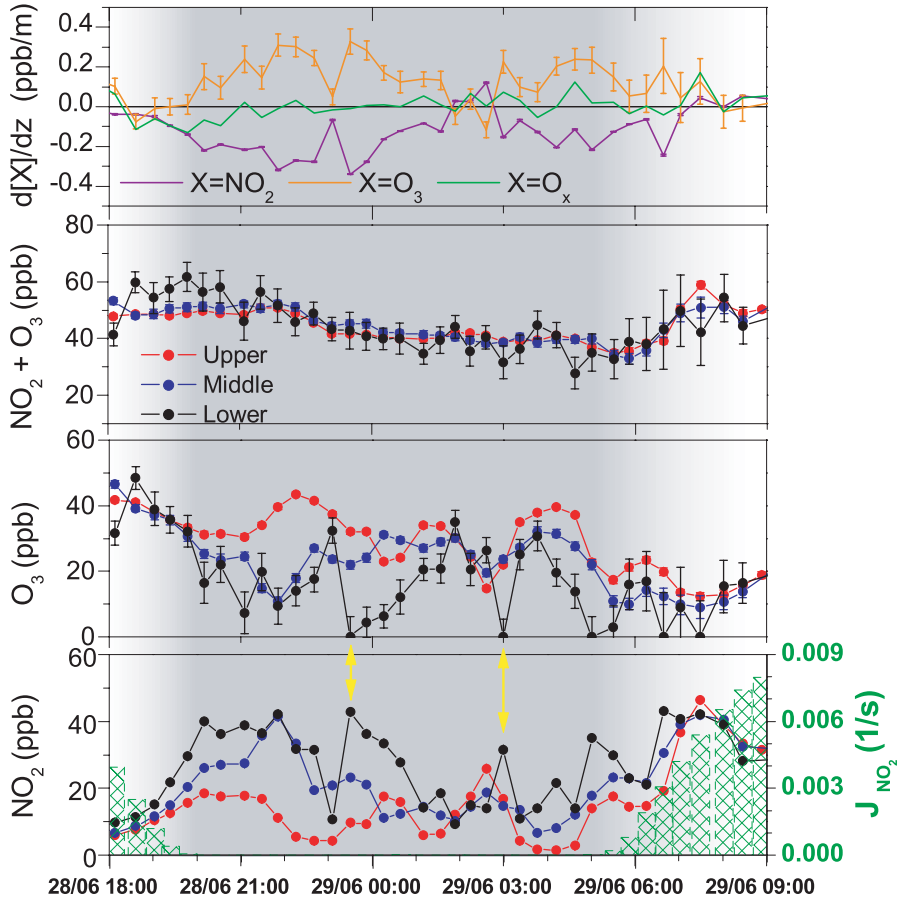

Fig. 9. Vertical profiles of NO_2 and O_3 on the night of 28 June–29 June 2001. The top panel shows the calculated vertical gradient of NO_2, O_3, and $O_x(O_3+NO_2)$ based on the upper and middle box data. The time series of J_{NO2}, photolysis frequency, indicates the time of sunset and sunrise.

calculated O_x level does not show a detectable gradient during most parts of the night. The variations in NO_2 and O_3 in the time series are canceled out in the sum and are not reflected in O_x levels. The only small variations of O_x around 03:00–05:00 are believed to be introduced by horizontal advection, becasue the in situ meteorological data on top of the different buildings show consistent wind directions during this night except for some deviations at 03:00–05:00.

Following sunrise, O_x levels increased, while O_3 concentrations remained low until 08:00 due to the large amount of freshly emitted NO during rush hour. This increase in O_x but not in O_3 was most likely caused by the high direct emissions of NO_2 by traffic and the downward transport of O_3 from the RL followed by (R1). After 08:00, NO_2 mixing ratios decreased with reduced traffic and continuously increasing photolysis rate. Both O_3 and O_x levels increased gradually as the photochemical O_3 formation process started to take over.

As stated earlier, surface NO emissions drive the height-dependent NO titration process. Because (R1) only converts O_3 to NO_2 without changing O_x levels, O_x should have no vertical gradient if (R1) is the dominant chemical process in determining vertical distributions of both NO_2 and O_3. Therefore, our observations in this scenario clearly demonstrate the dominant role of NO titration for the vertical variations of NBL chemistry during a typical polluted night in Phoenix. The similar anti-correlated profiles of NO_2 and O_3 were also observed in earlier studies at suburban areas with heavy traffic (Chen et al., 2002).

During the majority of the nights in this field campaign, negligible O_x gradients similar to those in Fig. 9 were observed. However, there were exceptions during two nights: 16 June–17 June and 30 June–1 July, which need further discussions.

4.2.2 Stronger surface emission case

During the night of 16 June–17 June (Fig. 10), which showed the strongest vertical gradients of trace gases during this two-week field study, the large vertical gradients of NO_2 and O_3

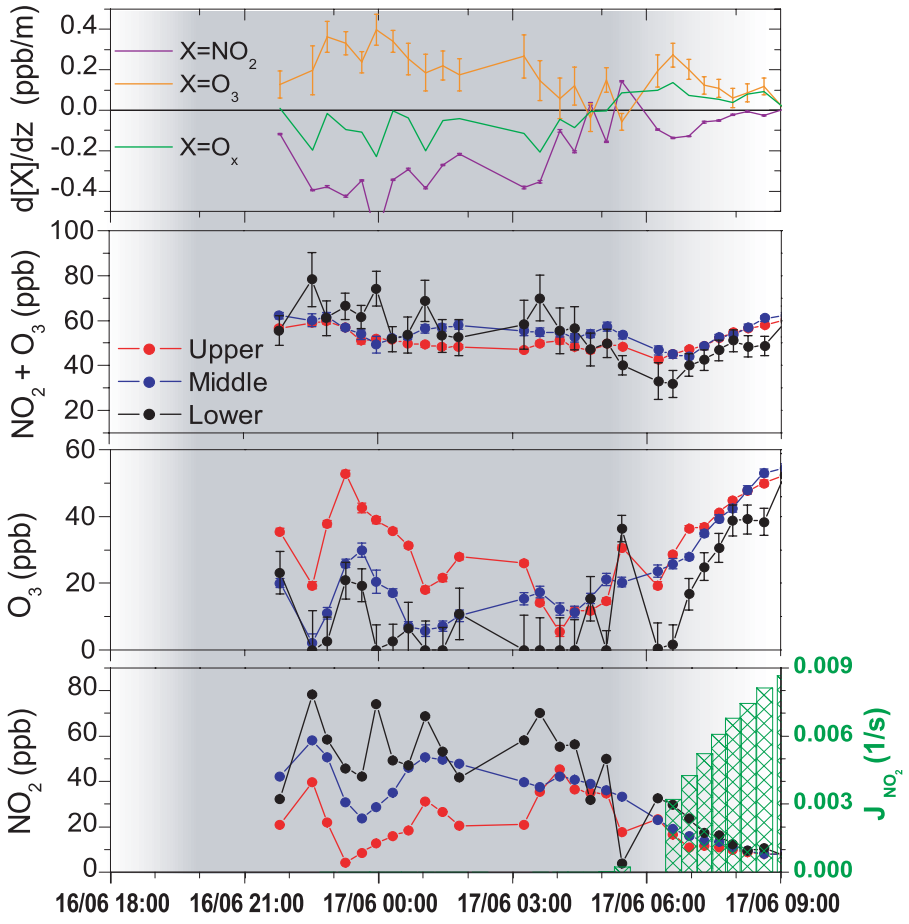

Fig. 10. Vertical profiles of NO_2 and O_3 on the night of 16 June–17 June 2001 (see caption of Fig. 9 for a more detailed explanation).

mostly canceled each other out as seen by the small O_x gradient. The O_x level in the lower box was, however, in general higher than that in the middle and upper boxes. As a result, the calculated O_x vertical gradient was negative during most parts of the night. Considering the very high NO_2 levels and the surface O_3 depletion during this night, it is believed that particularly high ground-level emissions are responsible for this negative O_x gradient.

Although NO emission rates were not directly monitored during this study, the mixing ratios of NO were measured at the ground level and on two floors of the BankOne building (Fig. 12). The night of 28 June–29 June, which showed the behavior of O_x profiles similar to those during most other nights in Phoenix (Sect. 4.2.1), was a typical weekday night. The evening traffic in the city led to up to 30 ppb NO at the ground. Due to the extremely high daytime temperature in summer, the morning rush hour in Phoenix often occurs as early as around sunrise. The morning NO peak in Fig. 12 shows the early rush hour with a maximum at about 06:00. The delay in the NO maximum at higher altitudes was caused by the slow upward transport of NO. In contrast, the night of 16 June–17 June was a weekend night, from Saturday to Sunday. The morning rush hour NO peak is absent. However, high NO mixing ratios at both the ground level and 50 m altitude were observed during this night (Fig. 12), which was caused by increased traffic due to a sports event in downtown Phoenix.

As a result of the exceptionally high nocturnal NO emissions during 16 June–17 June and the rapid reaction (R1), large amounts of O_3 were converted into NO_2 in the lower NBL. The lower box NO_2 reached as high as 80 ppb during this night, which is about twice the maximum NO_2 level of the previous case. A large NO_3 production rate by (R2) is thus expected. In fact, this was the night with the highest NO_3 levels during this experiment. Above 200 ppt NO_3 were detected in the upper box, while the average maximum NO_3 level during the other nights was below 100 ppt. Because of the very active NO_3-N_2O_5 chemistry, NO_2 formation pathways other than NO titration (R1), such as (R3) and (R5), significanlty influence the vertical distribution of O_x in the NBL. In particular, the downward transport of N_2O_5 and its thermal dissociation (R5) in the lower NBL can indirectly

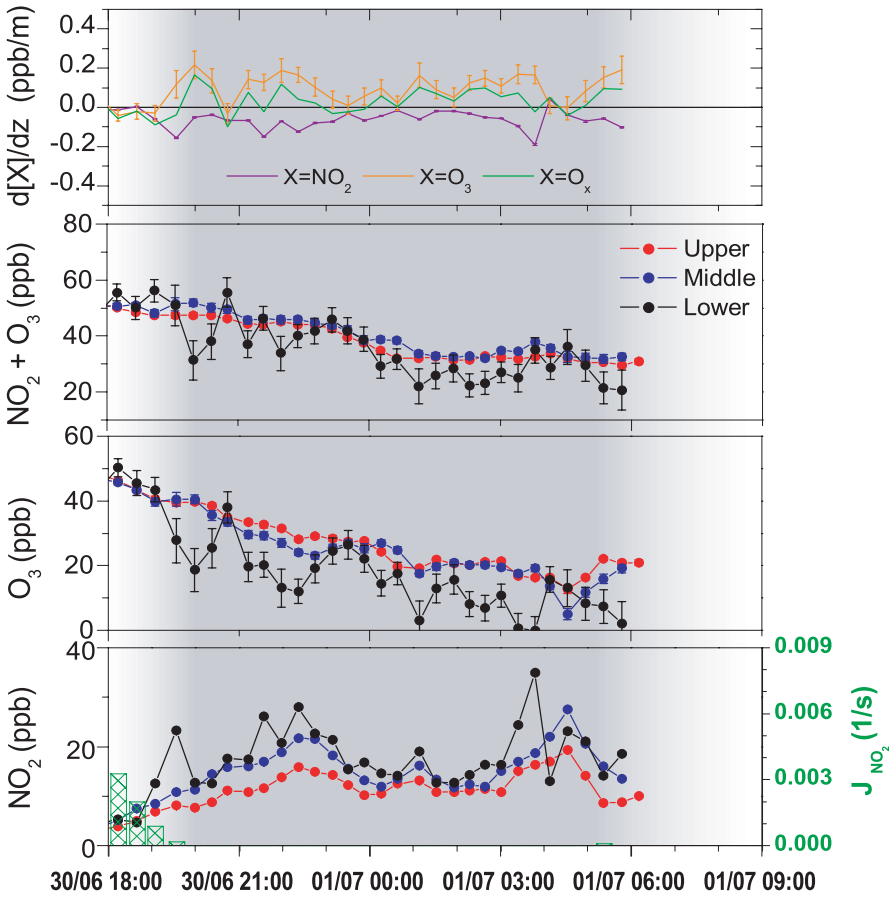

Fig. 11. Vertical profiles of NO_2 and O_3 on the night of 30 June–1 July 2001 (see caption of Fig. 9 for a more detailed explanation).

transport NO_2 and NO_3 from aloft to the surface (Geyer and Stutz, 2004a). Together with the rapid reaction of NO_3 with NO (R3), this mechanism leads to the formation of three NO_2 molecules for every N_2O_5 molecule transported downwards. With the particularly high NO_3 mixing ratios observed during this night (Fig. 10), N_2O_5 and its transport could contribute significantly to the high O_x levels close to the ground. The direct emission of NO_2 at the surface is often unimportant due to the low NO_2/NO_x emission ratio (Kurtenbach et al., 2002). Although, the emissions were particularly strong in this case, a larger NO_2 deposition on the ground surface could counter balance or even outweigh the direct NO_2 emissions. Therefore, direct emissions most likely contributed little to the observed O_x gradients. It should be noted that in this case dry deposition of O_3 is unimportant as a consequence of the high NO_x emissions and fast O_3 depletion. Instead, dry deposition of NO_2 became significant as an indirect O_3 loss. Again, this loss could be counter balanced by strong direct NO_2 emissions. Whether the overall effect due to dry deposition, direct NO_2 emissions, and vertical transport lead to a net sink or source for O_x in the NBL has to be discussed more quantitatively with the help of chemical transport models.

Nevertheless, the negative O_x vertical gradient during the night of 16 June–17 June shows that in cases of very high surface NO_x emissions, the dominance of the NO titration process is reduced and the idea of a constant vertical distribution of O_x does not hold.

4.2.3 Weaker surface emission case

In contrast, during the night of 30 June–1 July, another weekend night of Saturday to Sunday, the O_x levels remained at slightly smaller values in the lower box than those of the two higher boxes (Fig. 11). A positive O_x vertical gradient was present with values about half of the O_3 gradient.

Although horizontal advection cannot be completely excluded, a competitive O_x sink must be present near the surface, leading to the positive O_x gradient. Dry deposition of O_3, which is unimportant when strong NO titration dominates in a polluted area, is a major cause of surface O_3 removal in rural areas (Geyer and Stutz, 2004a). Theoretically it could also contribute considerably in an urban case with light NO emissions. The comparison of in situ NO data (Fig. 12) shows much lower NO levels on 30 June–1 July than the previous two cases. The lower box NO_2

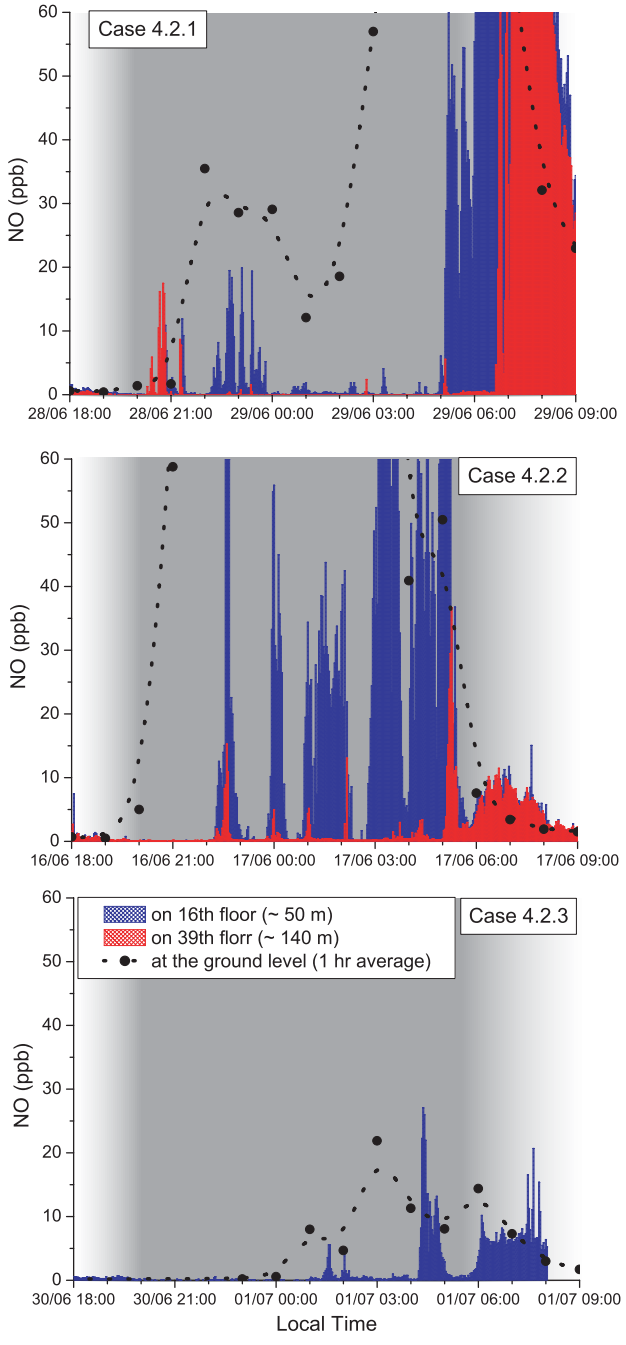

Fig. 12. Comparison of NO levels on nights of 16 June–17 June, 28 June–29 June and 30 June–1 July.

levels (Fig. 11) were only about half of those in the case of Sect. 4.2.1 (Fig. 9). In addition, the vertical gradients of both NO_2 and O_3 were also considerably smaller compared to the other cases. These observations all suggested weaker NO emissions during this night. The role of NO titration in the O_x vertical distribution is thus weakened. With considerable levels of O_3 at the bottom of the NBL, dry deposition competed with NO titration and resulted in an additional O_3 loss at the ground surface, which led to the lower total O_x level in the lower box than aloft. While dry deposition can be important for the O_x budget in urban areas, for example in this case, the fast NO titration causes the O_3 deposition velocity to change with height and thus makes the accurate estimation of this velocity for air pollution models challenging (Wesely and Hicks, 2000). It should be noted that NO_2 deposition and the resulting negative vertical flux to the ground surface was not considered in the above discussions.

4.2.4 Comparison of the gradients in different cases

The comparison of these three cases clearly demonstrates the critical role of the surface emission strength in influencing the vertical structures of nocturnal chemistry in urban environments. The significance of NO titration and consequently the vertical distribution of O_x vary with the surface emission strength.

It should be noted that besides the emission strength, the NBL stability also influences the vertical distribution of trace gases (see Sect. 3.3). Although the different surface emission strengths during these three nights ($E_{16\ \text{June}-17\ \text{June}} > E_{28\ \text{June}-29\ \text{June}} > E_{30\ \text{June}-1\ \text{July}}$), contributed to some extent, in determining the difference in the magnitude of NO_2 and O_3 vertical gradients $\left(\frac{dC}{dz}_{16\ \text{June}-17\ \text{June}} > \frac{dC}{dz}_{28\ \text{June}-29\ \text{June}} > \frac{dC}{dz}_{30\ \text{June}-1\ \text{July}}\right)$, the factor of atmospheric stability must be considered as well. As shown in Fig. 5, the night of 16 June–17 June was characterized by very low wind speed mostly around 0–2 m/s and a strong temperature inversion of up to 5 K difference between the roof of ADEQ (110 m) and Hilton (45 m). Meteorological data from the other two nights show weaker atmospheric stability. The night of 28 June–29 June had a little higher wind speed and a relatively weaker temperature inversion. The temperature difference between the two buildings was at most 2 K. During the night of 30 June–1 July, no temperature inversion was observed and the wind speed was mostly above 3 m/s. Therefore, the NBL stability during these cases has the same order as that of the emission factor (Table 4). The difference in both emissions and atmospheric stability determined the different gradient magnitudes during these nights. A quantitative discrimination of these two factors, however, requires future model studies.

Despite the above-discussed differences, the three cases do have clear common features in the trend of O_x. In all cases, O_x mixing ratios gradually decreased with the development of the night and reached the lowest values around sunrise. A detailed discussion of the O_x budget based on these data will be given in Sect. 4.5.

Table 4. Comparison of O_x loss during nights with different stabilities and different emissions.

	Stability	Emission	d[NO_2]/dt ppb/h	d[O_3]/dt ppb/h	d[O_x]/dt ppb/h
16 June–17 June	Strong	Strong	–	–	−1.4±0.3
28 June–29 June	Medium	Medium	–	–	−1.9±0.1
30 June–1 July	Weak	Weak	−0.2±0.1	−2.3±0.1	−2.6±0.1

4.3 NO_3 chemistry in the urban NBL

The chemistry of NO_3 and its reservoir species N_2O_5 has a strong influence on the fate of O_x. Due to the vertical distributions of NO_2 and O_3 and the height-dependent reaction (R2), NO_3 also develops vertical gradients. The observations in Phoenix generally showed high NO_3 levels often above 50 ppt in the upper box, but small and often negligible levels close to the ground (see Fig. 3 in Sect. 3.1).

Figure 7 shows NO_3 vertical profiles for the night of 26 June–27 June, which was already discussed in Sect. 3.3 with respect to the influence of stability on vertical profiles. During periods of high stability in the early and late night, clear positive vertical gradients of NO_3 can be identified, which is consistent with the model prediction by Geyer and Stutz (2004a) for polluted urban cases. NO_3 mixing ratios reached up to 150 ppt in the upper box and decreased towards the ground. During the period with low NBL stability, however, NO_3 levels were low (0–30 ppt) at all altitudes. The vertical gradients were less distinct than those during the stable periods, mainly due to the increased vertical mixing. To understand the cause for this NO_3 behavior, the height dependence of NO_3 formation and loss are investigated in the following. To avoid the influence of the scatter of the lower box data as a result of temporal variations in the path-integrated data and the large errors of the lower box mixing ratios, we will focus on the data in the middle and upper boxes.

The opposite vertical distributions of NO_2 and O_3 lead to an altitude dependence of NO_3 formation through (R2). The NO_3 production rate, $P_{NO3}=k_2\cdot[NO_2]\cdot[O_3]$ ($k_2=1.4\times10^{-13}e^{-2470/T}$cm^{3}s^{-1}; Atkinson et al., 2004), calculated based on measured mixing ratios of NO_2 and O_3, showed values about 0.5–1$\times10^7$ cm^{-3} s^{-1} during both stable and unstable periods (Fig. 7). The vertical gradient of P_{NO3} was weak and did not show a clear trend due to the opposite signs of O_3 and NO_2 gradients. However, a closer look at the dependence of P_{NO3} gradients on the NO_2 and O_3 distributions displays a systematic behavior of P_{NO3} profiles. Based on the important role of NO titration in typical urban areas (Sect. 4.2) and an assumption of linear vertical profiles of both NO_2 and O_3, P_{NO3} at altitude z can be estimated with the concentrations at a reference altitude (i.e., $[NO_2]z_0$ and $[O_3]z_0$) and the vertical gradients (δ=d[O_3]/dz≈−d[NO_2]/dz) of NO_3 precursors:

$$P_{NO3}(z) \approx k_2 \cdot ([NO_2]z_0 - \delta \cdot \Delta z) \cdot ([O_3]z_0 + \delta \cdot \Delta z) \quad (4)$$

The derivation of the vertical gradient of P_{NO3} reveals that the sign of the P_{NO3} gradient at a specific altitude is solely dependent on the comparison of NO_2 and O_3 concentrations. The product of the difference in $[NO_2]_z$ and $[O_3]_z$ levels and their vertical gradients δ determines the magnitude of the P_{NO3} gradient:

$$\begin{aligned}\frac{dP_{NO3}}{dz} &\approx k_2 \cdot \delta \cdot ([NO_2]z_0 - [O_3]z_0 - 2\delta \cdot \Delta z) \\ &\approx k_2 \cdot \delta \cdot ([NO_2]_z - [O_3]_z) \end{aligned} \quad (5)$$

Figure 7 shows generally lower NO_2 levels than those of O_3 in both upper and middle boxes. Consequently, P_{NO3} at these altitudes displayed a negative vertical gradient during most of the night. The largest gradient of P_{NO3} appeared when the NO_2 and O_3 profiles were strong (i.e., the high stability periods during 26 June–27 June) or when O_3 levels were considerably higher than those of NO_2 in the beginning of the night, which is also consistent with the expression of Eq. (5). In contrast, a very weak vertical gradient of P_{NO3} appeared during the period with low NBL stability as a result of a small δ in Eq. (5).

Despite the presence of a negative vertical gradient of the NO_3 production rate, positive NO_3 gradients were observed. We thus discuss the NO_3 sink and the consequent steady state lifetime of NO_3:

$$\tau_{NO3} = \frac{[NO_3]}{NO_3 \text{ loss or production rate}} = \frac{[NO_3]}{k_2 \cdot [NO_2] \cdot [O_3]} \quad (6)$$

It has to be noted that this calculation is based on the steady state assumption of both NO_3 and its reservoir species N_2O_5, which is not always fulfilled in the atmosphere (Brown et al., 2003). Its accuracy depends on the ambient NO_2 level, the temperature, the levels of species reacting with NO_3 directly, and the vertical transport of the reservoir species N_2O_5 which influences NO_3 distribution indirectly (Geyer and Stutz, 2004a). Here we use τ_{NO3} to gain insight into the general behavior of the altitude dependence of the loss processes of NO_3. A more precise analysis requires the use of a chemical transport model.

τ_{NO3} was considerably shorter in the lower NBL than aloft during times of high vertical stability on 26 June–27 June

(Fig. 7). It was in the range of 0–300 s for the middle box but reached 500–1200 s in the upper box. The much longer lifetimes in the upper box are clearly associated with the observed high NO_3 mixing ratios.

Due to the surface emissions and the negative vertical profile of NO (Sect. 4.2.1), the direct loss process of NO_3 through reaction (R3) is stronger near the ground. In particular, NO, the sink species of NO_3, is converted into NO_2 as it is transported upward and has very low mixing ratios at the top of the NBL, consequently leading to longer NO_3 lifetimes aloft. The reaction with various VOCs (R4), which are also emitted at the ground, could contribute to the fast NO_3 loss at the surface as well. The short NO_3 lifetime in the lower NBL, to a large extent, determined the low NO_3 mixing ratios even when a higher NO_3 production rate than aloft was present. Although aerosol uptake of N_2O_5 (R6) following the equilibrium (R5) is an indirect NO_3 loss, as will be further discussed below, the extremely low *RH* (Fig. 8) minimizes the influence of (R6) on the NO_3 distribution in Phoenix. In addition, a temperature inversion in the stable NBL (Fig. 8) affects the height profile of the reaction rates of (R5) due to the strong temperature dependence of the equilibrium between reactants and the product (Geyer and Stutz, 2004a). Higher temperatures at the top of the NBL can thus result in a considerable shift of the equilibrium to the direction of NO_3 and contributed to the strong positive NO_3 vertical gradient during the stable periods on 26 June–27 June.

During the weak stability period, τ_{NO3} was surprisingly low at all altitudes (Fig. 7). The highest $\tau_{NO3}$was only about 1 min. As indicated by the high wind speed (Fig. 8) and the weak vertical profiles of measured trace gases (Fig. 7), the vertical mixing during this period was strong. Ground-level emitted NO_3 sink species were transported upward efficiently and resulted in a rapid loss of NO_3 at all measured altitudes. Consequently the very short τ_{NO3} explains the particularly low NO_3 levels during this period despite a fairly constant P_{NO3} throughout the night.

In summary, the comparison of the NO_3 production rate and lifetime reveals that the positive NO_3 vertical gradients in urban areas are a consequence of the NO_3 loss that is more efficient near the ground. Neither NO_3 mixing ratio nor its atmospheric lifetime in the NBL can be determined based on ground-level measurements alone. These results support earlier model studies (Aliwell and Jones, 1998; Geyer and Stutz, 2004a) and suggest that calculations from ground measurements of NO_3 can lead to underestimation of the nocturnal oxidizing capacity of the atmosphere.

4.4 Vertical profiles of the reservoir species N_2O_5

The formation of N_2O_5 and its thermal decay (R5) result in a temperature dependent equilibrium between N_2O_5, NO_3, and NO_2. Ideally, in the absence of other N_2O_5 sinks (i.e., R6), the chemical steady state N_2O_5 concentration is determined by $K_{eq}(T)\cdot[NO_2]\cdot[NO_3]$, in which $K_{eq}(T)=5.5\times10^{-27}e^{10724/T}\mathrm{cm}^3$ (Wangberg et al., 1997). Due to the very low *RH* in Phoenix, the influence of (R6) on the steady state of N_2O_5 is rather unimportant. Based on this temperature dependent equilibrium, unique vertical profiles of chemical steady state N_2O_5 mixing ratios were derived with the measured data of NO_2 and NO_3 as well as the temperature profile (Fig. 7). The temperature measured on top of ADEQ was taken as the upper box temperature. The average temperature on top of ADEQ and Hilton was used as the middle box temperature.

During the stable periods on the night of 26 June–27 June, N_2O_5 mixing ratios reached up to 350 ppt, while they were below ~100 ppt during the unstable period, mainly because of the difference in NO_3 concentrations for different periods (see Sect. 4.3). N_2O_5 during the stable periods showed considerably higher levels in the middle box than in the upper box. This negative N_2O_5 vertical gradient was not reported in any earlier studies except in model calculations of a special urban case with very high ambient temperature (Geyer and Stutz, 2004a). The N_2O_5 profiles during the unstable period were weak and showed higher or equal N_2O_5 levels aloft than in the middle box, which is in agreement with the model results of most other scenarios (Geyer and Stutz, 2004a).

Based on the temperature dependent equilibrium, N_2O_5 vertical distribution is influenced by the opposite vertical distribution of NO_2 and NO_3 and the temperature profile. The maximum temperature inversion during this night (~2 K difference between top of Hilton and top of ADEQ) could lead to at most 12% decrease in N_2O_5 mixing ratios from the middle box to the upper box. The vertical variations of N_2O_5 during this night were, therefore, mainly caused by the opposite vertical distribution of NO_2 and NO_3.

Using an assumption of linear NO_2 and NO_3 distributions similar to the one used in the discussion of P_{NO3}, the N_2O_5 mixing ratio at altitude z can be expressed as $K_{eq}\cdot([NO_2]_{Z0}+\frac{d[NO_2]}{dz}\cdot\Delta z)\cdot([NO_3]_{Z0}+\frac{d[NO_3]}{dz}\cdot\Delta z)$. Neglecting the possible height dependence of $K_{eq}(T)$, one can derive the gradient of steady state N_2O_5 mixing ratios at a specific altitude:

$$\frac{\partial[N_2O_5]}{\partial z} \approx [N_2O_5]_z \cdot \left(\frac{\left(\frac{d[NO_3]}{dz}\right)}{[NO_3]_z} + \frac{\left(\frac{d[NO_2]}{dz}\right)}{[NO_2]_z} \right) = [N_2O_5]_z \cdot (A-B) \quad (7)$$

The sign of N_2O_5 gradient is thus determined by the sum of the relative vertical gradients of NO_3, A, and NO_2, −B (note that the relative vertical gradient of NO_2 is always negative), at the corresponding altitude. For example, during the stable period on 26 June–27 June, a low NO_2 concentration and a strong vertical gradient of NO_2 could result in a large value of term B in Eq. (7) while term A was relatively small due to the high NO_3 concentration. A negative N_2O_5 vertical gradient was thus determined. The high N_2O_5 concentrations during this period further magnified this negative gradient (Eq. 7).

In contrast, term B in Eq. (7) during the unstable period was much smaller as a result of higher NO_2 levels and weaker vertical gradients, while term A became relatively large due to the very low NO_3 levels. The resulting positive N_2O_5 vertical gradient was weak because of the low concentrations of N_2O_5 during these hours.

It should be noted that the vertical transport of N_2O_5 could influence the above-discussed steady state of N_2O_5 under some circumstances. The impact of transport on the calculated N_2O_5 distribution in Phoenix will be further investigated in a forthcoming paper using a 1-D chemical transport model.

Our studies show complex N_2O_5 vertical profiles in the NBL depending on a number of factors. Although the role of the aerosol uptake of N_2O_5 through (R6) is weakened in Phoenix due to the low *RH*, it can be an important atmospheric denoxification process which removes NO_3 and NO_2 and further an indirect loss of O_3 in other polluted areas with high *RH* and aerosol density. The N_2O_5 profile, together with the vertical distribution of aerosols, can thus play an important role in determining the altitude dependence of the NBL O_x sink in those cases.

4.5 Budgets of O_3, NO_2, and O_x in the NBL

As discussed in Sect. 4.1, nocturnal chemistry can influence O_3 levels for the following morning in polluted urban areas through its influence on the levels of total O_x (see Eq. 3). The nocturnal budgets of both O_3 and NO_2 thus play critical roles.

The dominant O_3 loss during night-time is the reaction of O_3 with freshly emitted NO (R1). The true influence of this reaction on the O_3 levels for the following morning is the shift in the Leighton ratio (see Eqs. 1–2 in Sect. 4.1). The other important loss processes of O_3 in the NBL include its reaction with NO_2 (R2) and its heterogeneous destruction, either on aerosols, $L_{O_3+\text{aerosol}}$, or the ground, $L_{O_3\text{dry dep}}$. Dry deposition of O_3 becomes particularly important in the case of low NO emissions (Sect. 4.2.3), but is negligible in heavily polluted areas where O_3 is already depleted at the ground (Sect. 4.2.2). In addition, the downward transport of O_3 from higher altitudes, VT_{O_3}, constitutes the only source of O_3 into the NBL. We can thus summarize the budget of O_3 in the NBL as:

$$\frac{d[O_3]}{dt} = -k_1 \cdot [O_3] \cdot [NO] - k_2 \cdot [O_3] \cdot [NO_2] - L_{O_3+\text{aerosol}} - L_{O_3\ \text{dry dep}} + VT_{O_3} \quad (8)$$

The main source of NO_2 in the urban NBL is its formation through (R1). Due to the low NO_2/NO_x emission ratio, NO_2 direct emission, E_{NO2}, generally plays a small role even when nocturnal emissions are particularly strong (for example, the case in Sect. 4.2.2). The formation of NO_3 (R2) is an NO_2 sink, while the loss of NO_3 through reaction with NO (R3) is another source of NO_2. The N_2O_5 chemistry is also both a source and a sink of NO_2. Thus the shift of the equilibrium of (R5) gives a measure of the impact of N_2O_5 on the nocturnal NO_2 budget. Direct heterogeneous uptake of NO_2 on aerosols, $L_{NO_2+\text{aerosol}}$, and dry deposition on the ground, $L_{NO_2\text{dry dep}}$, can also play a role. Finally the NBL NO_2 is lost by the upward transport to higher altitudes, VT_{NO_2}. The budget of NO_2 in the NBL is therefore given as:

$$\begin{aligned}\frac{d[NO_2]}{dt} = {} & k_1 \cdot [O_3] \cdot [NO] - k_2 \cdot [O_3] \cdot [NO_2] \\ & + 2k_3 \cdot [NO_3] \cdot [NO] \\ & + (k_{5-} \cdot [N_2O_5] - k_{5+} \cdot [NO_3] \cdot [NO_2]) \\ & - L_{NO_2+\text{aerosol}} - L_{NO_2\ \text{dry dep}} + E_{NO_2} - VT_{NO_2} \end{aligned} \quad (9)$$

Based on these considerations, one can set up an expression for the total O_x change in the NBL.

$$\begin{aligned}\frac{d[O_X]}{dt} = {} & -2 \cdot (k_2 \cdot [O_3] \cdot [NO_2] - k_3 \cdot [NO_3] \cdot [NO]) \\ & + (k_{5-} \cdot [N_2O_5] - k_{5+} \cdot [NO_3] \cdot [NO_2]) \\ & - L_{O_3+\text{aerosol}} - L_{O_3\ \text{dry dep}} - L_{NO_2+\text{aerosol}} \\ & - L_{NO_2\ \text{dry dep}} + E_{NO_2} + VT_{O_3} - VT_{NO_2} \end{aligned} \quad (10)$$

Assuming a chemical steady state of NO_3, the terms in the first parenthesis in Eq. (10) describe the net NO_3 loss that does not regenerate O_x (i.e., NO_3 loss through (R4) and the disequilibrium of (R5) as discussed in Sect. 4.1). Therefore, these terms can be replaced by $L_{NO_3+\text{VOC}}$ and $(k_{5+}\cdot[NO_3]\cdot[NO_2] - k_{5-}\cdot[N_2O_5])$. Considering a steady state assumption for N_2O_5, the latter is equivalent to the heterogeneous uptake and the vertical transport of N_2O_5. Assuming that N_2O_5 vertical transport only redistributes N_2O_5 but does not influence the total N_2O_5 budget in the NBL, the disequilibrium term, $(k_{5+}\cdot[NO_3]\cdot[NO_2] - k_{5-}\cdot[N_2O_5])$, is approximately equal to $L_{N_2O_5+\text{aerosol}}$.

For typical urban cases, Eq. (10) can be further simplified. Earlier studies show small influence of the aerosol uptake of both O_3 and NO_2 on the urban nocturnal budget of these species (Geyer and Stutz, 2004a). Considering the fact that dry deposition is determined by the ground level concentration of a species, the vertical exchange coefficient, and the reactive uptake coefficient, the dry deposition terms in Eq. (10) can be combined into $L_{O_x\text{dry dep}}$ assuming similar uptake coefficients of these two species. Vertical transport is an important loss and source of NBL NO_2 and O_3, respectively. Since the vertical gradients of O_3 and NO_2 are often of the same magnitude but opposite signs (see Sects. 3 and 4.2), the O_x loss due to the upward transport of NO_2 out of the NBL is as much as the O_x source through the downward transport of O_3 into the NBL (i.e., $VT_{NO_2}=VT_{O_3}$). The two terms in Eq. (10), $VT_{O_3}-VT_{NO_2}$, therefore cancel out. This also implies that vertical transport can be an important NO_2 source in the RL and influences the chemistry at higher altitudes.

Following these arguments, one can conclude that the budget of O_x in the NBL is dominated by the atmospheric

denoxification processes (i.e., $L_{N_2O_5+aerosol}$ and L_{NO_3+VOC}), the dry deposition of O_x, and the direct emission of NO_2:

$$\frac{d[O_X]}{dt} = -3 \cdot L_{N_2O_5+aerosol} - 2 \cdot L_{NO_3+VOC} - L_{Ox\,dry\,dep} + E_{NO_2} \quad (11)$$

It should be noted that the influence of N_2O_5 aerosol uptake ($L_{N_2O_5+aerosol}$), which is relatively unimportant for the chemical steady state of N_2O_5 in the dry atmosphere of Phoenix, is tripled in the total O_x loss rate and becomes an effective factor influencing the nocturnal budget of O_x.

We can now apply these theoretical considerations to the observations in Phoenix. To derive a picture averaged for the entire NBL, the original measurement results along the lower light path spanning 140–10 m altitudes, which are approximately equivalent to the integrated trace gas concentrations in the lowest 140 m of the atmosphere, are used for discussing the NBL O_x budget. We again use the nights discussed in Sect. 4.2, 16 June–17 June, 28 June–29 June, and 30 June–1 July, to show the influence of atmospheric stability and emissions on the total O_x budgets. A linear fit of the change of O_x concentrations along the lower light path from 20:00 (21:30 for the night of 16 June–17 June) until 04:00 was applied to determine the O_x loss rate averaged throughout the night (Table 4). While this procedure works well with O_x, it is less accurate for O_3 and NO_2 due to temporal variations. Figures 9 and 10 show large temporal variations of both NO_2 and O_3 levels during the night of 16 June–17 June and 28 June–29 June. The average rates of NO_2 and O_3 are thus difficult to estimate. Nevertheless, a linear fit was applied to get the O_3 and NO_2 change rates for the night of 30 June–1 July, during which the temporal variations are relatively weak (Fig. 11). The results in Table 4 show the comparison of the O_x loss rates during the three nights investigated here. Considering the magnitude of the error bars and the temporal variations, the difference in the total O_x loss during these nights is very small, despite the large difference in the meteorology and chemical conditions among these cases.

To understand this behavior, the factors determining the O_x budget in Eq. (11) have to be investigated separately. (1) Denoxification processes: The significance of denoxification strongly depends on the levels of N_2O_5 and NO_3. High NO_2 and O_3 levels lead to high production rate of NO_3 and thus N_2O_5. For example, the highest NO_3 levels in this two-week experiment were observed during the night of 16 June–17 June with the strongest emissions (see Sect. 3.2). Figure 3 also shows higher NO_3 and NO_2 on 16 June–17 June than those on 30 June–1 July, suggesting higher steady-state N_2O_5 levels on 16 June–17 June. The loss of O_x through denoxification is therefore larger in the first case. (2) Dry deposition: The significance of dry deposition is more difficult to estimate since it depends on both O_x levels and the vertical stability in the NBL. The O_3 deposition rate strongly decreases with the increase of surface NO emissions and the increase of vertical stability. The O_3 dry deposition during the night of 16 June–17 June is thus much smaller than during the other night since both stability and emission strengths are in favor of a smaller O_3 deposition rate, especially during the later part of this night when O_3 was depleted. Dry deposition of NO_2 is, however, only weakly dependent on the NBL stability because the effects of reduced NO_2 levels near the ground and faster transport toward the surface due to a better mixing balance each other (Geyer and Stutz, 2004a). The NO emission rate has a strong influence on the NO_2 deposition and thus leads to a larger $L_{NO_2dry\,dep}$ for the high emission night. The O_3 and NO_2 deposition rates thus change in different directions. The direct comparison of total O_x deposition rates during these two nights cannot be made due to limited data of the stability and emission rates. (3) Direct emission: Finally, the influence of direct NO_2 emissions is obviously stronger when surface NO_x emissions are higher (i.e., on the night of 16 June–17 June).

Based on these discussions, it can be concluded that the evaluation of O_x loss in the NBL requires considerations of all the terms determining the nocturnal O_x budget and thus can be very complex. The dry deposition term is especially difficult to evaluate and the contribution of O_3 and NO_2 needs to be treated separately for different conditions. Since the values of this term in urban scenarios modeled by Geyer and Stutz (2004a) are in the same order of magnitude as the average night-time O_x loss rate in our observations, dry deposition plays an important role in the behavior of total O_x change during these nights. It can be deduced that the combination of a larger loss rate by denoxification, a larger source rate by direction emission, and a most likely smaller O_x deposition rate during 16 June–17 June results in a similar total O_x loss rate for this night to that on 30 June–1 July.

It is interesting to note that the average O_3 loss rate during the night of 30 June–1 July was very close to the total O_x loss rate. NO_2 levels did not show clear change throughout the night. A considerable NO_2 loss rate through vertical transport as a result of a weak stability most likely balanced the small NO_2 source rate due to the low nocturnal emissions. Therefore the influence of NBL chemistry on morning BL O_3 levels for this case is mostly the result of the nocturnal O_x loss. The influence caused by nocturnal emissions through the shift of Leighton Ratio (see Eq. 2 in Sect. 4.1) is negligible. This conclusion can be further confirmed by the calculation of the ultimate O_3 loss as a result of the total O_x loss and the change of NO_x for this night (Table 5). Based on the interpretation of linear fit results discussed in Table 4, the O_x and NO_2 levels at about 19:30 (right before sunset) and 05:30 (right after sunrise) are estimated. The corresponding NO levels are evaluated based on in situ measurements. Therefore, without the impact of any other factors such as early morning convections, the total O_x and total NO_x change in the NBL are estimated to be -26 ppb and 2 ppb, respectively. Using Eq. (1) and the estimated O_x and NO_x levels, O_3 mixing ratios right before sunset and right

Table 5. Evaluation of the ultimate O_3 loss during the night of 30 June–1 July.

	$[O_x]$ from interpreted DOAS data	$[NO_2]$ from interpreted DOAS data	[NO] from in situ data	$[O_3]$ from Eq. (1)
19:30	48 ppb	16 ppb	1 ppb	31 ppb
05:30	22 ppb	14 ppb	5 ppb	4 ppb
	$\Delta[O_x]$	$\Delta[NO_x]$		$\Delta[O_3]$
19:30–05:30	−26 ppb	2 ppb		−27 ppb

after sunrise are calculated to be 31 ppb and 4 ppb, giving a 27 ppb ultimate reduction of the O_3 level. Assuming a constant NO_x level, one can derive the ultimate O_3 loss caused by only O_x loss through nocturnal chemistry to be 25 ppb, which contributes 92% to the ultimate O_3 loss. The influence of nocturnal emissions (i.e., the increase of total NO_x levels) is rather small ($\sim$2 ppb) for this weakly polluted case.

In contrast, during the heavily polluted night of 16 June–17 June, the nocturnal O_x loss is relatively smaller and thus contributed less to the ultimate O_3 removal. NO_x levels could increase considerably as a result of the strong NO emission followed by (R1) and the direct emission of NO_2. The strong NBL stability that led to ineffective upward transport of NO_x out of the NBL could also contribute to the NO_x increase by reducing the NO_x loss term. Consequently, the contribution of the shift of Leighton Ratio (see Eq. 2) to the ultimate O_3 loss is more significant for this heavily polluted case. Unfortunately a quantitative evaluation is not possible for this night as a result of the temporal variations in NO_2 and O_3 levels and the missing data in the early evening.

The comparison of O_x loss for these different cases suggests that the influence of nocturnal chemistry on O_3 levels in the next morning by changing total O_x levels in the NBL (see Eq. 3) can be similar in cases with different emissions and stability. The nocturnal NO emission followed by (R1), which only redistribute NO_2 and O_3 without changing total O_x and influence the morning O_3 levels through its influence on the Leighton Ratio, is however more important in heavily polluted areas (see Eq. 2).

5 Conclusions

Strong positive vertical gradients of O_3 and NO_3 and negative vertical gradients of NO_2, HONO and HCHO in the stable NBL were observed in the downtown area of Phoenix. The magnitudes of the gradients were significantly larger than in various earlier observations in rural or suburban areas due to the higher night-time ground-level emissions. The major features of the measured profiles are consistent with the concept of the night-time trapping of local pollutants in a stable NBL. The details of the interaction of processes involved in this chemistry system with vertical transport are, however, complex, depending on many factors. The following conclusions were drawn from our observations.

– The distinctive vertical distributions of reactive species compose a complex height-dependent nocturnal chemical system. Consequently, the atmospheric lifetimes of reactive species, the oxidative capacity of the NBL, the atmospheric denoxification process, and the O_3 production potential in the early morning boundary layer are strongly height-dependent.

– Vertical stability has a strong influence on the distribution of all trace gases in urban environments. Fast changes in vertical stability, as shown by the change in temperature gradients during the night and the onset of vertical mixing in the morning were observed to redistribute trace gases throughout the boundary layer.

– NO titration, as shown by the vertical profiles of NO_2, O_3 and O_x, plays a dominant role for the chemistry in the NBL. The surface emission strength of NO is a critical factor governing the magnitude and the shape of the vertical profiles.

– Vertical profiles of NO_3, are predominately caused by the short steady-state lifetime of NO_3 at the ground as a result of the fast reactions with ground-level emitted NO. NO_3 production rates, which demonstrated complicated vertical profiles depending on the distribution of both NO_2 and O_3, have a weaker influence.

– Calculated steady state N_2O_5 concentration showed unique vertical profiles, which are a function of the ambient temperature and the distribution of NO_2 and NO_3. These vertical profiles, together with possible aerosol profiles, lead to vertical variations of the aerosol uptake of N_2O_5, an indirect NO_3 loss and an important atmospheric denoxification process.

– O_x levels decreased gradually throughout all nights. The removal of O_x proceeds mainly through denoxification (i.e., NO_3+VOC reactions and N_2O_5 uptake) and dry deposition. Dry deposition on the ground is often not important in strongly polluted urban cases due to the low ground level O_3. However, elevated NO_2 levels in

these cases lead to larger NO_2 deposition. The total nocturnal O_x loss was observed to be of similar magnitude during nights with different emission strength, which is believed to be the result of the balance between a decreased dry deposition loss and an increased O_x source (i.e., direct NO_2 emissions) as the surface emissions increase.

– Ozone loss in the NBL proceeds through the loss of O_x and the impact of nocturnal NO emissions on the photostationary state in the morning. The latter is expected to be relatively more important in heavily polluted urban areas. It should be noted that this conclusion does not consider the influence of elevated NO_x on photochemical ozone formation that starts a few hours after sunrise.

These vertical variations of nocturnal chemistry, especially for urban cases with strong surface emissions, are often not considered well in many atmospheric chemistry field experiments or current air quality modeling studies. The results of our observations show strong impact of these variations on the morning chemistry and suggest that vertically highly resolved chemical-transport models, which include the quantitative determination of vertical transport of various trace gases, are necessary to accurately describe the budgets of O_3, NO_2, and many other trace gases in the stable NBL.

Acknowledgements. We gratefully acknowledge the support of the Department of Energy, grant DE-FG03-01ER63094 and the atmopsheric chemistry program of the National Science Foundation, award ATM–0348674. The assistance of Arizona Department of Environmental Quality is greatly appreciated. We would also like to thank C. W. Spicer from Battelle Columbus Operations for the in-situ measurements on BankOne, J. D. Fast and C. C. Doran from Pacific Northwest National Laboratory for providing meteorological data, C. Berkowitz, and R. Redman for their help in establishing the measurement site.

Edited by: A. Richter

References

Abram, J. P., Creasey, D. J., Heard, D. E., Lee, J. D., and Pilling, M. J.: Hydroxyl radical and ozone measurements in England during the solar eclipse of 11 August 1999, Geophys. Res. Lett., 27, 3437–3440, 2000.

Alicke, B., Platt, U., and Stutz, J.: Impact of nitrous acid photolysis on the total hydroxyl radical budget during the LOOP/PIPAPO study in Milan, J. Geophys. Res., 107, 8196, 2002.

Aliwell, S. R. and Jones, R. L.: Measurements of tropospheric NO_3 at midlatitude, J. Geophys. Res., 103, 5719–5727, 1998.

Aneja, V. P., Mathur, R., Arya, S. P., Li, Y., Murray, G. C., and Manuszak, T. L.: Coupling the vertical distribution of ozone in the atmospheric boundary layer, Environ. Sci. Technol., 34, 2324–2329, 2000.

Atkinson, R., Baulch, D. L., Cox, R. A., Crowley, J. N., Hampson, R. F., Hynes, R. G., Jenkin, M. E., Rossi, M. J., and Troe, J.: Evaluated kinetic and photochemical data for atmospheric chemistry: Volume I – gas phase reactions of O_x, HO_x, NO_x and SO_x species, Atmos. Chem. Phys., 4, 1461–1738, 2004, http://www.atmos-chem-phys.net/4/1461/2004/.

Aumont, B., Chervier, F., and Laval, S.: Contribution of HONO sources to the $NO_x/HO_x/O_3$ chemistry in the polluted boundary layer, Atmos. Environ., 37, 487–498, 2003.

Brown, S. S., Stark, H., and Ravishankara, A. R.: Applicability of the steady state approximation to the interpretation of atmospheric observations of NO_3 and N_2O_5, J. Geophys. Res., 108, 4539–4548, 2003.

Chen, C., Tsuang, B., Tu, C., Cheng, W., and Lin, M.: Wintertime vertical profiles of air pollutants over a suburban area in central Taiwan, Atmos. Environ., 36, 2049–2059, 2002.

Colbeck, I. and Harrison, R. M.: Dry deposition of ozone: some measurements of deposition velocity and of vertical profiles to 100 meters, Atmos. Environ., 19, 1807–1818, 1985.

Cros, B., Fontan, J., Minga, A., Helas, G., Nganga, D., Delmas, R., Chapuis, A., Benech, B., Druilhet, A., and Andreae, M. O.: Vertical profiles of ozone between 0 meters and 400 meters in and above the African Equatorial Forest, J. Geophys. Res., 97, 12 877–12 887, 1992.

Dentener, F. J. and Crutzen, P. J.: Reaction of N_2O_5 on tropospheric aerosols: Impact on the global distributions of NO_x, O_3, and OH, J. Geophys. Res., 98, 7149–7163, 1993.

Doran, J. C., Berkowitz, C. M., Coulter, R. L., Shaw, W. J., and Spicer, C. W.: The 2001 Phoenix Sunrise Experiment: vertical mixing and chemistry during the morning transition in Phoenix, Atmos. Environ., 37, 2365–2377, 2003.

Fast, J. D., Doran, J. C., Shaw, W. J., Coulter, R. L., and Martin, T. J.: The evolution of the boundary layer and its effect on air chemistry in the Phoenix area., J. Geophys. Res., 105, 22 833–22 848, 2000.

Fast, J. D., Torcolini, J. C., and Redman, R.: Pseudovertical temperature profiles and the urban heat island measured by a temperature datalogger network in Phoenix, Arizona, J. Appl. Meteorol., 44, 3–13, 2005.

Finlayson-Pitts, B. J. and Pitts, J. N.: Chemistry of the upper and lower atmosphere: theory, experiments and applications, Academic Press, San Diego; London, 2000.

Finlayson-Pitts, B. J., Wingen, L. M., Sumner, A. L., Syomin, D., and Ramazan, K. A.: The heterogeneous hydrolysis of NO_2 in laboratory systems and in outdoor and indoor atmospheres: An integrated mechanism, Phys. Chem. Chem. Phys., 5(2), 223–242, 2003.

Fish, D. J., Shallcross, D. E., and Jones, R. L.: The vertical distribution of NO_3 in the atmospheric boundary layer, Atmos. Environ., 33, 687–691, 1999.

Friedeburg, C., Wagner, T., Geyer, A., Kaiser, N., Vogel, B., Vogel, H., and Platt, U.: Derivation of tropospheric NO_3 profiles using off-axis differential optical absorption spectroscopy measurements during sunrise and comparison with simulations, J. Geophys. Res., 107, 4168–4195, 2002.

Galbally, I.: Some measurements of ozone variation and destruction in the atmospheric surface layer, Nature, 218, 456–457, 1968.

Garland, J. A. and Branson, J. R.: The mixing height and mass balance of SO_2 in the atmosphere above Great Britain, Atmos. Environ., 10, 353–362, 1976.

Geyer, A., Alicke, B., Mihelcic, D., Stutz, J., and Platt, U.: Compar-

ison of tropospheric NO_3 radical measurements by differential optical absorption spectroscopy and matrix isolation spin resonance, J. Geophys. Res., 104, 26 097–26 105, 1999.

Geyer, A. and Stutz, J.: Vertical profiles of NO_3, N_2O_5, O_3, and NO_x in the nocturnal boundary layer: 2. Model studies on the altitude dependence of composition and chemistry, J. Geophys. Res., 109, D12 307, doi:10.1029/2003JD004211, 2004a.

Geyer, A. and Stutz, J.: The vertical structure of OH-HO_2-RO_2 chemistry in the nocturnal boundary layer: a one-dimentional model study, J. Geophys. Res., 109, D16 301, doi:10.1029/2003JD004425, 2004b.

Glaser, K., Vogt, U., and Baumbach, G.: Vertical profiles of O_3, NO_2, NO_x, VOC, and meteorological parameters during the Berlin Ozone Experiment (BERLIOZ) campaign, J. Geophys. Res., 108, 8253–8266, 2003.

Gusten, H., Heinrich, G., and Sprung, D.: Nocturnal depletion of ozone in the upper Rhine Valley, Atmos. Environ., 32, 1195–1202, 1998.

Harrison, R. M., Holmann, C. D., McCartney, H. A., and McIlvern, J. F. R.: Nocturnal depletion of photochemical ozone at a rural site, Atmos. Environ., 12, 2021–2026, 1978.

Hov, O.: One-dimensional vertical model for ozone and other gases in the atmosphere boundary layer, Atmos. Environ., 17, 535–550, 1983.

Jenkin, M. E. and Clemitshaw, K. C.: Ozone and other secondary photochemical pollutants: chemical processes governing their formation in the planetary boundary layer, Atmos. Environ., 34, 2499–2527, 2000.

Kleinman, L., Lee, Y.-N., Springston, S. R., Nunnermacker, L., Zhou, X., Brown, R., Hallock, K., Klotz, P., Leahy, D., Lee, J. H., and Newman, L.: Ozone formation at a rural site in the southeastern United States, J. Geophys. Res., 99, 3469–3482, 1994.

Kurtenbach, R., Ackermann, R., Becker, K. H., Geyer, A., Gomes, J. A. G., Lorzer, J. C., Platt, U., and Wiesen, P.: Verification of the contribution of vehicular traffic to the total NMVOC emissions in Germany and the importance of the NO_3 chemistry in the city air, J. Atmos. Chem., 42, 395–411, 2002.

McKendry, I. G., Steyn, D. G., Lundgren, J., Hoff, R. M., Strapp, W., Anlauf, K., Froude, F., Martin, J. B., Banta, R. M., and Olivier, L. D.: Elevated ozone layers and vertical down-mixing over the lower Fraser Valley, BC, Atmos. Environ., 31, 2135–2146, 1997.

Meller, R. and Moortgart, G. K.: Temperature dependence of the absorption cross sections of formaldehyde between 223 and 323 K in the wavelength range 225–375 nm, J. Geophys. Res., 201, 7089–7101, 2000.

Neu, U., Kunzle, T., and Wanner, H.: On the relation between ozone storage in the residual layer and daily variation in near-surface ozone concentration – A case study, Boundary Layer Meteorology, 69, 221–247, 1994.

Pisano, J. T., McKendry, I., Steyn, D. G., and Hastie, D. R.: Vertical nitrogen dioxide and ozone concentrations measured from a tethered balloon in the lower Fraser Valley, Atmos. Environ., 31, 2071–2078, 1997.

Sadanaga, Y., Matsumoto, J., and Kajii, Y.: Photochemical reactions in the urban air: Recent understandings of radical chemistry, J. Photochem. Photobio. C – Photochem. Rev., 4, 85–104, 2003.

Sander, S. P.: Temperature dependence of the NO_3 absorption spectrum, J. Phys. Chem., 90, 4135–4142, 1986.

Smith, G. D., Molina, L. T., and Molina, M. J.: Measurement of radical quantum yields from formaldehyde photolysis between 269 and 339 nm, J. Phys. Chem. A, 106, 1233–1240, 2002.

Stockwell, W. R., Kirchner, F., Kuhn, M., and Seefeld, S.: A new mechanism for regional atmospheric chemistry modeling, J. Geophys. Res., 102, 25 847–25 879, 1997.

Stutz, J. and Platt, U.: Numerical analysis and estimation of the statistical error of differential optical absorption spectroscopy measurements with least-squares methods, Appl. Opt., 35(30), 6041–6053, 1996.

Stutz, J., Kim, E. S., Platt, U., Bruno, P., Perrino, C., and Febo, A.: UV-visible absorption cross sections of nitrous acid, J. Geophys. Res., 105, 14 585–14 592, 2000.

Stutz, J., Alicke, B., and Neftel, A.: Nitrous acid formation in the urban atmosphere: Gradient measurements of NO_2 and HONO over grass in Milan, Italy, J. Geophys. Res., 107, 8192–8207, 2002.

Stutz, J., Alicke, B., Ackermann, R., Geyer, A., Wang, S., White, A. B., Williams, E. J., Spicer, C. W., and Fast, J. D.: Relative humidity dependence of HONO chemistry in urban areas, J. Geophys. Res., 109, 3307–3318, 2004a.

Stutz, J., Alicke, B., Ackermann, R., Geyer, A., White, A., and Williams, E.: Vertical profiles of NO_3, N_2O_5, O_3, and NO_x in the nocturnal boundary layer: 1. Observations during the Texas Air Quality Study 2000, J. Geophys. Res., 109, D12 306, doi:10.1029/2003JD004209, 2004b.

Van Dop, H., Guicherit, R., and Lanting, R. W.: Some measurements of the vertical distribution of ozone in the atmospheric boundary layer, Atmos. Environ., 11, 65–71, 1977.

Voigt, S., Orphal, J., and Burrows, J. P.: The temperature and pressure dependence of the absorption cross-sections of NO_2 in the 250–800 nm region measured by Fourier-transform spectroscopy, J. Photochem. Photobiol. A – Chem., 149, 1–7, 2002.

Wangberg, I., Etzkorn, T., Barnes, I., Platt, U., and Becker, K. H.: Absolute determination of the temperature behavior of the NO_2+NO_3+(M)↔N_2O_5+(M) equilibrium, J. Phys. Chem. A, 101, 9694–9698, 1997.

Wesely, M. L. and Hicks, B. B.: A review of the current status of knowledge on dry deposition, Atmos. Environ., 34, 2261–2282, 2000.

Zhang, J. and Rao, S. T.: The role of vertical mixing in the temporal evolution of ground-level ozone concentrations, J. Appl. Meteorol., 38, 1674–1691, 1999.